Journal Pre-proofs

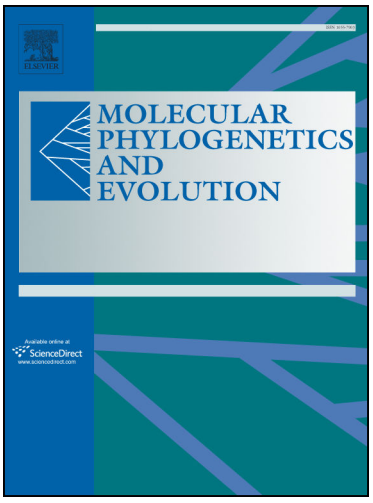

How challenging RADseq data turned out to favor coalescent-based species tree inference. A case study in Aichryson (Crassulaceae)

Philipp Hühn, Markus S. Dillenberger, Michael Gerschwitz-Eidt, Elvira Hörandl, Jessica A. Los, Thibaud F.E. Messerschmid, Claudia Paetzold, Benjamin Rieger, Gudrun Kadereit

PII: S1055-7903(21)00275-X
DOI: https://doi.org/10.1016/j.ympev.2021.107342
Reference: YMPEV 107342

To appear in: *Molecular Phylogenetics and Evolution*

Received Date: 3 July 2020
Revised Date: 5 July 2021
Accepted Date: 29 October 2021

Please cite this article as: Hühn, P., Dillenberger, M.S., Gerschwitz-Eidt, M., Hörandl, E., Los, J.A., Messerschmid, T.F.E., Paetzold, C., Rieger, B., Kadereit, G., How challenging RADseq data turned out to favor coalescent-based species tree inference. A case study in Aichryson (Crassulaceae), *Molecular Phylogenetics and Evolution* (2021), doi: https://doi.org/10.1016/j.ympev.2021.107342

How challenging RADseq data turned out to favor coalescent-based species tree inference.

A case study in Aichryson (Crassulaceae)

Philipp Hühn[1,2], Markus S. Dillenberger[2,3], Michael Gerschwitz-Eidt[2], Elvira Hörandl[4], Jessica A. Los[1], Thibaud F.E. Messerschmid[1,2,5], Claudia Paetzold[4,6], Benjamin Rieger[2] and Gudrun Kadereit[4]*

[1]Institute of Molecular Physiology (iMP), Johannes Gutenberg-University Mainz, Germany; [2]Institute of Organismic and Molecular Evolution (iOME), Johannes Gutenberg-University Mainz, Germany; [3]Institut für Biologie, Systematische Botanik und Pflanzengeographie, Freie Universität Berlin, Germany; [4]Department of Systematics, Biodiversity and Evolution of Plants, Georg-August-University Göttingen, Germany; [5]Lehrstuhl für Systematik, Biodiversität & Evolution der Pflanzen, Ludwig-Maximilians-Universität München, Germany; [6]Department of Botany and Molecular Evolution, Senckenberg Research Institute and Natural History Museum Frankfurt am Main, Germany;

**Correspondence to be send to: Lehrstuhl für Systematik, Biodiversität & Evolution der Pflanzen, Ludwig-Maximilians-Universität München, Germany;*

G.Kadereit@lmu.de

Declarations of interest: none

Running head.— RADseq data favor coalescent-based species tree inference

Keywords.— [clustering threshold selection, coalescent-based summary method, data bias, locus filtering, RADseq, species tree inference]

Abstract.— Analysing multiple genomic regions while incorporating detection and qualification of discordance among regions has become standard for understanding phylogenetic relationships. In plants, which usually have comparatively large genomes, this is feasible by the combination of reduced-representation library (RRL) methods and high-throughput sequencing enabling the cost effective acquisition of genomic data for thousands of loci from hundreds of samples. One popular RRL method is RADseq. A major disadvantage of established RADseq approaches is the rather short fragment and sequencing range, leading to loci of little individual phylogenetic information. This issue hampers the application of coalescent-based species tree inference. The modified RADseq protocol presented here targets ca. 5,000 loci of 300-600nt length, sequenced with the latest short-read-sequencing (SRS) technology, has the potential to overcome this drawback. To illustrate the advantages of this approach we use the study group *Aichryson* Webb & Berthelott (Crassulaceae), a plant genus that diversified on the Canary Islands. The data analysis approach used here aims at a careful quality control of the long loci dataset. It involves an informed selection of thresholds for accurate clustering, a thorough exploration of locus properties, such as locus length, coverage and variability, to identify potential biased data and a comparative phylogenetic inference of filtered datasets, accompanied by an evaluation of resulting BS support, gene and site concordance factor values, to improve overall resolution of the resulting phylogenetic trees. The final dataset contains variable loci with an average length of 373nt and facilitates species tree estimation using a coalescent-based summary approach. Additional improvements brought by the approach are critically discussed.

Abbreviations:

BSC – between-sample-clustering

CA-ML – maximum likelihood analysis of concatenated loci

CB-SM – coalescent-based summary method

CT – clustering threshold

gCF – gene concordance factor

GTEE – gene tree estimation error

HTS – high throughput sequencing

ILS – incomplete lineage sorting

ISC – in-sample-clustering

ML – maximum likelihood

MSC – multi-species coalescent (model)

NPL – new polymorphic loci

PE – paired-end

PIC – parsimony informative character

PIS – parsimony informative site

RADseq – restriction site-associated DNA sequencing

REase – restriction endonuclease

RRL – reduced-representation library (methods)

sCF – site concordance factor

SNP – single nucleotide polymorphism

SRS – short-read sequencing

SVD – SVDquartets

VAR – variable sites (sequence variation)

var – variability (VAR/locus length/number of samples)

1. INTRODUCTION

Resolving phylogenetic relationships of recently and rapidly radiating species complexes is a challenge because first, standard markers using universal primers are too conserved and fail to provide sufficient information, and second, inferring relationships is often complicated due to incomplete lineage sorting (ILS), hybridization/introgression and gene duplication/loss events (Pamilo and Nei, 1988; Maddison, 1997; Maddison and Knowles, 2006; Kubatko and Degnan, 2007; Whitfield and Lockhart, 2007; Degnan and Rosenberg, 2006, 2009; Heled and Drummond, 2009; Yang and Rannala, 2010; Rannala et al., 2020). Since different parts of the genome can have different evolutionary backgrounds, approaches analyzing multiple genomic regions have become the baseline for resolving such challenging lineages. The multi-species coalescent (MSC) model provides a natural framework for species tree inference that accounts for gene tree discordance due to ILS. However, full-coalescence approaches under the MSC are computationally very intensive when applied on large-scale genomic data and thus often not feasible (McCormack et al., 2013a; Smith et al., 2014; Zimmermann et al., 2014). Other approaches, such as maximum likelihood analysis of concatenated multi-locus data (de Queiroz et al., 1995; Yang 1996; de Queiroz and Gatesy 2007), coalescent-based summary methods that estimate species trees from independently inferred gene trees (here called “locus trees”) (Mirarab et al., 2014a; Mirarab and Warnow, 2015; Rannala et al., 2020) or coalescent-based methods that use site patterns of assembled loci for species tree inference (Bryant et al., 2012; Chifman and Kubatkto, 2014; Bryant and Hahn, 2020), became increasingly popular and widely used. Despite their popularity, these methods each have advantages and disadvantages and their correct application to modern high-throughput data, in particular approaches that generate short loci with high amounts of missing data such as RADseq, is highly controversial.

High-throughput sequencing (HTS) technologies and lab workflows for sample preparation improved enormously during the last decade and provide the opportunity to generate extensive datasets for phylogenetic inference (reviewed in Good, 2012; Reuter et al., 2015; Andrews et al., 2016; Mardis, 2017; McKain et al., 2018). Some of the most popular sample preparation protocols are grouped under the term reduced-representation library (RRL) preparation protocols, which are often combined with short-read sequencing (SRS). These methods target only a reduced subset of the studied genome for sequencing, therefore reducing computational complexity during assembly and analysis, facilitating a deeper sequencing depth per locus while increasing the number of samples included. The combination of both HTS and RRL enable simultaneous acquisition of genomic data of hundreds up to thousands of loci from dozens to hundreds of samples for systematic researchers and extend the questions and taxa that can be investigated tremendously. Widely used RRL approaches are hybridization capturing methods, e.g., on-array capture or in-solution capture (Mamanova et al., 2010), Hyb-Seq (Weitemier et al., 2014), targeted sequence capture (Grover et al., 2012) and restriction-site associated DNA sequencing (RADseq; Miller et al., 2007; Baird et al., 2008). The term RADseq comprises several methods that all rely on the enzymatic digestion of genomic DNA for complexity reduction, followed by adapter ligation, further reduction by size selection (either direct or indirect) and high-throughput sequencing (reviewed in Andrews et al., 2016). The cross-over approach hyRAD by Suchan et al. (2016) combines RADseq with capturing using either biotinylated DNA- or RNA-probes (Schmid et al., 2017; Suchan, 2018) obtained from the enzymatically fragmented DNA resources of the target group itself. Yet, the lab workflow is quite complex and time consuming. Thanks to the modular principle of RADseq, the individual wet lab steps, restriction endonucleases (REase/s) and adapters can be modified as required (see also McCormack et al., 2013b; Andrews et al., 2016; McKain et al., 2018; Parchman et al., 2018). This flexible toolbox of cheap, fast and individually scalable wet lab modules, as well as the

fact that no prior genomic information is required, paved the way for the success of RADseq methods in various fields of evolutionary research, particularly in non-model organisms (e.g., Eaton and Ree, 2013; Escudero et al., 2014; Harvey et al., 2016; Herrera and Shank, 2016; Razkin et al., 2016; de Oca et al., 2017; Dillenberger and Kadereit, 2017; Hamon et al., 2017; Curto et al., 2018; Wagner et al., 2018; Gerschwitz-Eidt and Kadereit, 2019; Paetzold et al., 2019; Rancilhac et al., 2019; Hipp et al., 2020; Karbstein et al., 2020; Wagner et al., 2020; Buono et al., 2021).

Despite these obvious benefits of RADseq, the approach poses some inherent challenges regarding the wet lab workflow, sequence assembly, data set processing and the application of coalescent-based species tree inference. Characteristically, RADseq datasets comprise relatively short loci (typically 100–250nt) and a high proportion of missing data (Ree and Hipp, 2015; Andrews et al., 2016; Eaton et al., 2017; Lee et al., 2018; McKain et al., 2018). The average fragment length obtained (and locus length assembled) depends on the degree of genomic reduction, which in turn depends on the REase/s chosen, the selected size segregation window and the genome size of the study group. To some extent, missing data (absence of data or missingness) in RADseq data is inherently expected due to mutations of the REase-specific recognition sites (Rubin et al., 2012; Eaton et al., 2017; Lee et al., 2018). Technical causes for missingness include: varying DNA quantity and quality, size selection artifacts, PCR bias or low sequencing depth and quality. All of these factors influence the average information content per locus and the uniformity with which it is distributed across taxa, consequently limiting the applicability of inference methods (Gatesy and Springer, 2014; Xi et al., 2015; Xu and Yang, 2016; Eaton et al., 2017; Sayyari et al., 2017; Lee et al., 2018; Molloy and Warnow, 2018).

RADseq is particularly appealing for studying non-model taxa, as large genome-sized datasets can be generated quickly and cost-effectively and assembled without requiring a

reference genome. However, *de novo* assembly and data processing can also be a major challenge. The bioinformatics effort related to RADseq data is often not straightforward and can heavily impact the assembly outcome regarding differentiation of orthologs and paralogs, as well as the quantity of recovered loci, sequence variation (VAR), single nucleotide polymorphisms (SNPs) and parsimony informative sites (PIS), respectively (Rubin et al., 2012; Ilut et al., 2014; Harvey et al., 2015; Shafer et al., 2017; Lee et al., 2018). To facilitate data processing, assembly pipelines such as Stacks (Catchen et al., 2013), dDocent (Puritz et al., 2014) and *ipyrad* (Eaton and Overcast, 2020) have been developed. These pipelines implement several main steps. 1) In-sample-clustering (ISC), in which reads within each sample are grouped by sequence similarity into putative loci. 2) Consensus calling of allele sequences from clustered reads. 3) Between-sample-clustering (BSC) of consensus sequences of all loci across all samples are clustered by sequence similarity to generate putatively homologous loci. 4) Data filtering based on given thresholds such as the number of samples per locus required (locus coverage) or the maximum proportion of shared heterozygous sites in a locus (detection of potential paralogs). To determine which reads represent the same genomic locus, a clustering threshold (CT) based on sequence similarity is used. Yet, genetic variation within the target genomes and across the studied taxa makes it difficult to find an appropriate CT (Rubin et al., 2012; Catchen et al., 2013; Hirsch and Buell, 2013; Ilut et al., 2014; Harvey et al., 2015; Ilut et al., 2014; Paris et al., 2017; Shafer et al., 2017; Lee et al., 2018; McCartney-Melstad et al., 2019). Both over- and undermerging are major issues in RADseq datasets, affecting ISC and BSC and therefore the resulting datasets. To ensure the homology of the assembled loci (Springer and Gatesy, 2018; McCartney-Melstad et al., 2019; Fernández et al., 2020; Simion et al., 2020), detailed evaluations of dataset metrics are used to find balanced dataset-specific CTs for ISC and BSC (e.g. Ilut et al., 2014; Mastretta-Yanes et al., 2015; McKinney et al., 2017; Paris et al., 2017; McCartney-Melstad et al., 2019). Approaches to facilitate this problem aim at the determination of suitable CTs for homology

assessment by analyzing trends of several assembly metrics over a wide range of tested CTs (hereafter referred to as "CT selection approach"). This is accomplished by plotting the metrics as a function of the CT range and searching for a region that avoids over- and undermerging areas and that provides an accurate clustering for the majority of loci (hereafter referred to as "transition zone"). This transition zone is assumed to minimize the assembly of paralogs, to maximize the yield of sequence variation, and to form the smallest distance among taxa (Ilut et al., 2014; Mastretta-Yanes et al., 2015; McCartney-Melstad et al., 2019). In other words: an informed selection of dataset-specific CTs yields maximum phylogenetic information with minimum missingness and least paralogs. Still, such CT selection approaches have to be taken with care because 1) the determined CT (for ISC and BSC) can never represent all taxa equally well and 2) all other chosen assembly parameters affect the outcome (Shafer et al., 2017; McCartney-Melstad et al., 2019).

Phylogenetic inference of assembled RADseq data presents the next challenge because the data properties often limit the choice of methods. Added to this is an ongoing, intense debate on the utilization of phylogenetic inference methods. The focus is mainly on: 1) the statistical consistency under the MSC, 2) the evolutionary framework to which the methods are applied (e.g. hybridization, horizontal gene transfer, ILS), and 3) the estimation accuracy under varying dataset conditions (e.g. linkage, phylogenetic information content, missingness, homology of data), leading to constant re-analyses and comparisons of simulated and empirical data to proof the diverging concepts (e.g. de Queiroz and Gatesy 2007; Edwards et al., 2007, 2016; Kubatko and Degnan 2007; Degnan and Rosenberg, 2009; Leaché and Rannala, 2011; Song et al., 2012; Bayzid and Warnow, 2013; Wu et al., 2013; Gatesy and Springer, 2013, 2014; Springer and Gatesy 2014, 2016, 2018; Mirarab et al., 2014a,b, 2015, 2016; Chou et al., 2015; Roch and Steel 2015; Mendes and Hahn, 2018; Molloy and Warnow, 2018; Bryant and Hahn, 2020; Rannala et al., 2020). This somewhat amusing and abstruse debate, with sometimes remarkably tailored data for proof, complicates the search for

appropriate phylogenetic inference methods for RRL-SRS data. Fact is that the locus properties are pivotal for selecting appropriate species tree inference methods. Due to the short fragment length, RADseq loci are generally assumed to lack sufficient phylogenetic information to generate locus trees as input for coalescent-based summary methods (Rubin et al., 2012; Gatesy and Springer, 2014; Xi et al., 2015; Hosner et al., 2016; Molloy and Warnow, 2018).

Gene-tree-based coalescent methods (summary methods; hereafter referred to as CB-SM) are a favorable choice for phylogenetic inference of rather long and informative loci (Mirarab et al., 2014a, 2015; Vachaspati and Warnow, 2015; Xu and Yang, 2016; Molloy and Warnow 2018; Rannala et al., 2020). CB-SM infer species trees by a two-step system: individual gene trees are estimated, and their summary statistics are then used as data input for species tree estimation. While CB-SM are becoming popular for their ability to handle large amounts of data in a short time, they are best known for their sensitivity to gene tree estimation error (GTEE). When applied to datasets composed of short loci of little individual phylogenetic information and a high proportion of missingness, as is characteristic of RADseq datasets, the effect on estimation accuracy can get quite severe (Chou et al., 2015; Roch and Warnow, 2015; Xi et al., 2015; Xu and Yang, 2016; Sayyari et al., 2017; Molloy and Warnow, 2018). Therefore, the focus on the effects of filtering loci for specific properties prior to gene and species tree estimation is becoming increasingly relevant (e.g. Lanier et al., 2014; Chen et al., 2015; Xi et al., 2015; Hosner et al., 2016; Huang and Knowles 2016; Simmons et al., 2016; Sayyari et al., 2017; Molloy and Warnow 2018).

Coalescent-based site-based methods are another option for species tree inference (Bryant et al., 2012; Chifman and Kubatko, 2014; Xu and Yang, 2016). Such approaches bypass the generation of locus trees by generating the species tree directly from all given site patterns, thus avoid the issue of GTEE. The sites are required to have individual histories or at

least very little linkage. Violation of this assumption leads to a statistically inconsistent species tree estimate (Bryant et al., 2012; Chifman and Kubatko 2014; Xu and Yang, 2016). Under certain challenging data conditions, site-based methods were found to be more accurate than gene tree-based summary (Chou et al., 2015; Long and Kubatko, 2018; Molloy and Warnow, 2018).

RADseq data are most commonly analyzed using maximum likelihood analysis of a concatenated supermatrix (hereafter referred to as CA-ML) (Yang, 1996; de Queiroz and Gatesy, 2007; Rubin et al., 2012). In case of CA-ML, several thousand loci are treated as one locus that evolved under a single evolutionary history. This is violating the MSC and may theoretically lead to poorly resolved, incomplete, or positively misleading species tree estimates (Degnan and Rosenberg, 2006, 2009; Kubatko and Degnan, 2007; Knowles, 2009; Roch and Steel, 2015, Xu and Yang, 2016; Mendes and Hahn, 2018; Rannala et al., 2020). In addition, bootstrapping is also commonly performed across the entire supermatrix, potentially resulting in spuriously high support values caused by the sheer dataset size (Kubatko and Degnan, 2007; Kumar et al., 2012; Rubin et al., 2012; Liu et al., 2015; Wang et al., 2017, Minh et al., 2020a). Still, it also has been shown that CA-ML can be comparably or more accurate than coalescent-based methods under various conditions of linkage, locus length, information content, missingness, ILS and GTEE (Mirarab et al., 2014a; Chou et al., 2015; Roch and Warnow, 2015; Mirarab et al., 2016; Springer and Gatesy, 2016; Long and Kubatko, 2018; Molloy and Warnow, 2018).

Despite the ongoing debate about the pros and cons of approaches to sequence generation, data assembly, phylogenetic inference, and, the assumption that RAD data do not favor coalescent-based summary methods, we think there is a need to take advantage of the significant methodical progress made in the last decade and explore their potential for

practical use. Our objective is to test whether longer RADseq loci enable coalescent-based species tree inference, and to provide advice on how to handle and analyze challenging data.

We modified several modules of the RADseq toolbox to obtain a library containing a small number of fragments (ca 5,000 assembled loci), with lengths of ca. 300-600nt, sequenced with the latest SRS technology (Illumina MiSeq v3 kit, 300nt PE) and applied this protocol (Fig. 1) to the plant genus *Aichryson* Webb & Berthel. (Crassulaceae), a rapidly radiated yet relatively small genus distributed in Macaronesia, for which standard sanger sequenced markers failed to provide a resolved phylogeny (Fairfield et al., 2004). The data analysis (Fig. 2) included a CT selection approach to facilitate an informed choice of suitable CTs for ISC and BSC during *de novo* assembly (Fig. 3) and an exploratory approach to determine the properties of the assembled loci, with respect to locus coverage (missingness), locus variability (phylogenetic information) and locus length, and thus their suitability as input for CB-SM (Fig. 4). We compared the phylogenetic outcome of this assembly using CA-ML (RAxML by Stamatakis, 2014), CB-SM (ASTRAL III by Zhang et al., 2018) and put it in perspective to the site-based approach SVDquartets by Chifman and Kubatko (2014). To assess the phylogenetic results, we also evaluated the resulting BS support values relative to gene and site concordance factors that were calculated using IQ-TREE (Minh et al., 2020a, b).

2. MATERIALS AND METHODS

2.1 Study group, sampling and DNA extraction

Together with *Monanthes* Haw. and *Aeonium* Webb & Berthel., *Aichryson* belongs to the Macaronesian tribe Aeonieae of the Crassulaceae family (Eggli, 2008). The genus comprises 15 species with the centre of diversity on the Canary Islands (11 species; Bañares, 2002, 2015a, 2017), three species on Madeira, and one species on the island of Santa Maria in the Azores (Moura et al., 2015). *Aichryson* is divided into two sections, sect. *Aichryson* and sect. *Macrobia* Webb & Berthel. Section *Macrobia* includes only *Aichryson tortuosum* (Aiton) Webb & Berthel., a perennial, small shrub endemic to Lanzarote (subsp. *tortuosum*) and Fuerteventura (subsp. *bethencourtianum* Botte & Bañares). All other species belong to sect. *Aichryson* and are monocarpic, mostly annual herbaceous plants (Bañares, 2015a). Within sect. *Aichryson* several natural hybrids are described (Bañares 2015b). *Aichryson* proved to be monophyletic and likely sister to *Monanthes icterica* (Webb ex Bolle) Christ in molecular phylogenetic studies on Aeonieae based on cp markers and ITS (Mort et al., 2002; Fairfield et al., 2004). The genus comprises both diploid and tetraploid species (Uhl, 1961; Suda et al., 2005).

We sampled a total of 29 individuals representing 14 species of *Aichryson* (only *A. santa-mariensis* M.Moura, Carine & M.Seq. is missing) and two accessions of *Monanthes icterica* as outgroup (Supplementary Table 1, "sampling"). For 20 samples we were able to assess the ploidy level on a CyFlow cytometer (PARTEC) using the isolation buffer "OTTO I" (2.1 g Citric-acid-1-hydrat, 10 ml 5% Triton X-100, 90 ml ddH_2O). FloMax v2.8.2 (QA GmbH, Münster, Germany) was used for the particle analysis and the measurement of the peaks (Table S1, "flow cytometry"). For the remaining samples, published ploidy levels were incorporated (Uhl, 1961; Suda et al., 2005).

DNA-extraction was conducted using the DNeasy Plant Mini-Kit (QIAGEN, Venlo, Netherlands) according to the manufacturer's protocol for "Purification of Total DNA from Plant Tissue (Mini Protocol)" with a number of modifications outlined in the online Appendix 1. The DNA concentration and quality were evaluated using a NanoDrop 1000 Spectrophotometer (Thermo Fisher Scientific, Waltham, MA, USA), a Qubit 3.0 Fluorometer (Thermo Fisher Scientific, Waltham, MA, USA) and gel electrophoresis.

2.2 In silico digestion, restriction enzyme choice and adapter design

The search for suitable restriction enzymes for our approach was performed *in silico* and based on 1) the desired fragment length (300-600nt), 2) the number of samples per library (up to 50), 3) the expected sequencing output of the MiSeq v3 kit (up to 25 Million), and 4) the targeted sequencing depth (aimed at ~10× per fragment), leading to the required fragment yield of 5,000 within the target length range. Initially we tested commonly used REases individually. However, the REases tested did not meet our requirements, thus we tested combinations of two REases each. For this, we have taken into account a minimum length of 6nt for the recognition site and the simultaneous applicability of two REases in a single reaction. The *in silico* digestion was performed using the software CLC genomics Workbench v9.5.5 (Qiagen) with its included "Restriction Site Analysis" for several genomes of various focal groups including *Beta vulgaris* L., Amaranthaceae (BioProject PRJNA41497) and *Kalanchoe fedtschenkoi* Raym.-Hamet & H.Perrier, Crassulaceae (BioProject PRJNA397334). The resulting restriction maps were evaluated with respect to fragments showing two cut sites within the desired length window of 300-600nt. Among other suitable REase combinations, the REases *BamHI* (G'GATCC) and *KpnI* (GGTAC'C) best met our criteria for a double digest (for excerpts of the REase selection, see also Supplementary Table S2, "in silico digest"). In case of *Aichryson*, the *in silico* digest of the distantly (yet closest) related *K. fedtschenkoi* genome (divergence to Aeonieae is roughly 58.60 [44.60–73.62] mya,

Messerschmid et al., 2020), resulted in 61,692 fragments, of which 4,429 fragments fell in the targeted length range.

In contrast to widely established strategies (Elshire et al., 2011; Peterson et al., 2012; Andrews et al., 2016), we aimed at sequencing all generated fragment types, including fragments framed by identical restriction motifs. Thus, we designed the barcode and common adapters for both REases motifs (Table S2, "BamHI adapter", "KpnI adapter"). The barcode sequences were obtained from Elshire et al. (2011) and van Gurp (2017). Both barcode and common adapter fit to the overhang of the *BamHI* and *KpnI* cut sites (Fig. 1b). We were able to achieve the set aim with this design, however, we recommend a more flexible adapter/indexing strategy that accounts for technical bias during wet lab and sequencing (e.g. MacConaill et al., 2018; Bayona-Vásquez et al., 2019).

2.3 RADseq

The major changes compared to other RADseq approaches such as ddRADseq (Peterson et al., 2012) or Genotyping by Sequencing (GBS; Elshire et al., 2011) are: the usage of two rare cutter REases that produce c. 5,000 fragments within a target range of 300-600nt (Fig. 1a), adapters binding to all generated fragments (Fig. 1b), an extended size selection range (Fig. 1d) and an extra size selection step during the final purification (Fig. 1f). In particular the two size selections were important to fully exploit the sequencing range (see also Appendix 1, Fig. A1.6, A1.7). Since the RADseq toolbox includes many modifiable modules, various protocols might be capable of generating libraries/datasets of an extended length range and we encourage an impartial testing of this potential (see also: McCormack et al., 2013b; Andrews et al., 2016; McKain et al., 2018; Parchman et al., 2018). The following is a brief overview of the workflow. For the detailed protocol, see Appendix 1 and Supplementary Table S3.

314 *2.3.1 RADseq lab workflow*

315 We used 200ng genomic DNA as input for the double digest reaction (Fig. 1a), which
316 was followed by adapter ligation (Fig. 1b) in the same reaction tube. For thorough saturation
317 of cut sites, 6µl adapter working solution (0.5ng/µl) containing equimolar amounts each motif
318 pair were used. Reactions were incubated for 3 hours at 37°C, respectively. The libraries were
319 multiplexed using 100ng DNA each (Fig. 1c), followed by a column-based cleaning of the
320 pool. Size selection (Fig. 1d) was performed using Pippin Prep (Sage Science, Beverly, MA,
321 USA) with a segregation range of 350-720nt. The size-selected products were amplified using
322 a low-cycle 2-step PCR protocol (Fig. 1e). Subsequently, PCR products were collected in
323 three pools (Table S3), purified and quantified. Final purification, accompanied by the 2nd size
324 segregation, was done using the NucleoMag NGS kit (Macherey-Nagel, Düren, Germany)
325 with a ratio of 0.8 bead suspension to one part library. The purified library was resuspended in
326 25 µl Buffer AE for sequencing.

327 *2.3.2 Library quality assessment and sequencing*

328 Library quality was validated by measuring the DNA concentration by Qubit
329 Fluorometer and assessing the fragment distribution by Bioanalyzer electropherogram
330 (Appendix 1). Sequencing was performed on an Illumina MiSeq (San Diego, CA, USA;
331 Reagent Kit v3 600-cycle) at StarSEQ (Mainz, Germany) producing 300nt PE reads in three
332 different runs (Supplementary Table S4).

333 *2.4 Data assembly*

334 *2.4.1 Raw sequence treatment*

335 Raw data quality was assessed with FastQC 0.11.4 (Andrews, 2010; Fig 2a; Table S4
336 "run I-III"). Raw reads were demultiplexed (Table S2 and S3) using *ipyrad* v0.9.52 (Eaton
337 and Overcast, 2020) twice, once for each REase cut site (Fig. 2a). This two-fold

demultiplexing was necessary due to the motifs occurring on both read directions. The fastq-files were combined and adapter sequences were removed with Cutadapt 1.18 (Martin, 2011). FastQC reports of the demultiplexed/adapter trimmed samples were combined using MultiQC v1.9 (Ewels et al., 2016; Table S4 "mean quality scores").

2.4.2 ipyrad

We used *ipyrad* v0.9.52 (Eaton and Overcast, 2020) for *de novo* RADseq assembly. Several filtering parameters of the *ipyrad* pipeline (v9 or above, Eaton and Overcast 2020) represent percentages, allowing the application of the selected thresholds to variable read lengths and thus supporting clustering of datasets obtained by a broad sequencing range. We used default parameters, except for the ones outlined below.

2.4.3 Assembly parameter settings

The de-multiplexed samples were split into two groups according to ploidy level (di- or tetraploid; Table S1). The diploid dataset contained nine *Aichryson* samples, the tetraploid dataset contained 18 *Aichryson* and two *Monanthes icterica* samples. Parameter #18 (max_alleles_consens) was set to two and four, respectively (Supplementary Table S5). With respect to the extended read length, we allowed up to 24 indels per locus (parameter #23). We assumed increased gene flow and set parameter #24 to 0.7 (Bañares, 2015b; max_Hs_consens). Parameters #11 and #12, which give the minimum depth for statistical and majority rule base calling, were set to 10. We aimed at an average cluster depth (avg_depth_mj) of >20× for statistical base calling (Pamilo et al., 2011; Eaton and Overcast, 2020).

2.4.4 Selection of suitable clustering thresholds for ISC and BSC

Avoiding both, over- and undermerging of putative loci is not trivial in high-throughput datasets. If the selected CT is too lax, paralogous reads will be incorrectly clustered and

treated as orthologs (overmerging) and if the selected CT is too strict, reads belonging to an actual locus will incorrectly be split into several loci (undermerging) with low variability (Supplementary Figure S1.A). To determine suitable CTs for ISC and BSC, we used several CT selection approaches as guidance (Ilut et al., 2014; Mastretta-Yanes et al., 2015; Paris et al., 2017; McCartney-Melstad et al., 2019) and defined the assumptions to determine suitable CTs. 1) Over- and undermerging ranges have to be identified to avoid merging/splitting effects within these areas. 2) Overmerging is indicated by highly heterozygous clusters/alleles with a high proportion of filtered paralogs (Ilut et al., 2014; McCartney-Melstad et al., 2019). Hence, a suitable CT is expected in an increasing area of heterozygosity and a decreasing area of flagged paralogs, between the maxima of both metrics. 3) Undermerging of orthologs leads to an increased number of loci (and lower locus coverage in ISC, lower sample coverage per locus in BSC) while sequence divergence among taxa decreases (Mastretta-Yanes et al., 2015; McCartney-Melstad et al., 2019). Thus, sequence variation declines while missingness increases. A suitable CT is expected near a steep increase in number of clusters/loci and amount of missingness while heterozygosity is biologically realistic (ISC) and locus variability is high (BSC).

To prevent introducing a potential bias due to ploidy, we split the samples into two groups (di- and tetraploid) for ISC assembly (*ipyrad* assembly steps 1-5, Fig. 2b). Following ISC CT selection, all samples were merged for BSC (*ipyrad* assembly steps 6 and 7). A CT range of 0.81-0.99 (in 0.01 increments) was tested. To assess the abovementioned criteria for CT selection, we plotted a variety of metrics as a function of the tested CT range as box- and scatter plots (see also Figure S1.B and S1.C). For the ISC CT selection, we evaluated the number of clusters (clusters_total), the average read depth (avg_depth_total), the number of filtered paralogs (filtered_by_maxH) and the heterozygosity. For the BSC CT selection, we additionally evaluated the number of retained loci, sequence variation (VAR, SNPs and PIS) and proportion of missingness (sequences_missing). In addition, we calculated the “new

polymorphic loci" (NPL) in order to detect the assembly containing most accurately clustered sequence variation, which is indicated by the so-called "hockey stick signal" (Paris et al., 2017). We expected the transition zone from over- to undermerging to be characterized by trend changes, e.g. prominent differences in the medians of adjacent CTs and compressions or expansions of the quartiles (in boxplots) or changes in the slope intensity (in scatter plots). Multiple suitable CTs within a transition zone of a metric and across metrics were averaged to determine a consensus CT.

2.4.5 Processing of the unfiltered ipyrad assembly

The *ipyrad* loci-file of the unfiltered "raw" assembly was parsed with a custom Perl script (available on GitHub https://github.com/philipphuehn/RADseq-locus-filtering) for the specific locus ID, the length, the number of samples, SNPs and PIS (VAR in total) and the proportion of missingness for each locus (Fig. 2c "parsing of locus properties"). We used BLAST+ 2.7.1 (Camacho et al., 2009) to identify chloroplast loci by blasting all loci against four reference plastomes from the Crassulaceae (GenBank accessions: *Sedum uniflorum* subsp. *oryzifolium* (Makino) H.Ohba: NC_027837, *Sedum sarmentosum* Bunge: NC_023085, *Phedimus takesimensis* (Nakai) 't Hart: NC_026065, *Phedimus kamtschaticus* (Fisch. & C.A.Mey.) 't Hart: NC_037946). Loci of a plastid origin as well as loci showing no parsimony informative sites were removed (Fig. 2c, "0 PIS + cp loci removal"). In addition, this "raw" assembly was used for initial phylogenetic inference and clade definition to compare potentially different phylogenetic results from subsequently filtered datasets (see 3.4.1).

2.5 Locus filtering and dataset selection

In general, phylogenetic inference by CB-SM is very sensitive to GTEE, which most often is caused by loci showing little sequence variation, high missingness or fractional coverage (Chou et al., 2015; Roch and Warnow, 2015; Xi et al., 2015, 2016; Xu and Yang, 2016; Sayyari et al., 2017; Hosner et al., 2016; Lee et al., 2018; Molloy and Warnow, 2018).

We filtered the here generated RADseq loci into several sub-datasets to test for a potential influence of locus properties on phylogenetic inference (Fig. 2c, "locus filtering"). First, we determined the impact of the locus properties on CB-SM reconstruction (see 2.5.1). This filtering approach suggested a potential impact of biased phylogenetic signal due to non-randomly distributed partial taxon coverage (Sanderson et al., 2010, 2011, 2015; Simmons, 2012; Xi et al., 2015; 2016; Hosner et al., 2016; Sayyari et al., 2017; Dobrin et al., 2018). This so-called "biased missingness" has been shown to cause high GTEE, thus results in conflicting, unsupported locus trees and consequently in a decline of species tree estimation performance (Xi et al, 2015, 2016; Hosner et al., 2016; Sayyari et al, 2017; Molloy and Warnow, 2018). We therefore performed a second locus filtering with respect to locus length and evaluated phylogenetic patterns of CB-SM and CA-ML reconstructions (see 2.5.2). The locus filtering scripts are available at GitHub (https://github.com/philipphuehn/RADseq-locus-filtering).

2.5.1 Locus filtering by coverage, variability, length intervals and dataset selection based on average missingness

The loci were filtered with respect to the average variability (var=VAR/locus length/number of samples; "min_var"), minimum number of samples per locus (number of samples/locus; "min_samples"), and locus length intervals ("length_int") and rearranged to new sub-datasets (Fig. 2c, "locus filtering", Supplementary Table S6). For the "min_var" sub-datasets, seven thresholds were used (0.01, 0.25, 0.50, 0.75, 1.0, 2.0, 3.0, "min_var_001" – "min_var_300"). Six thresholds by increments of four were used for the "min_samples" sub-datasets (4, 8, 12, 16, 20, 24, "min_samples_4" – "min_samples_24"). The locus length interval datasets were created based on eight intervals starting from the minimum length to 250nt, and then ranging by 50nt steps from 251nt to 550nt, and 551nt to the maximum length ("int_min-250" – "int_551-max"). Properties of these datasets, such as the total number of

loci, VAR, SNPs, PIS (average per locus), sample coverage/missingness, and average locus length were recorded (Fig. 2c, "sub-dataset properties summary"). For each rearranged sub-dataset, ML locus trees were estimated and used for CB-SM inference (see 2.6.2). We recorded the bootstrap support values of all branches of each tree and assigned them to three categories: backbone, clade and within clade branch support values. Clade branches contained all samples of the defined clades (see 3.4.1 for clade definition). All support values within the defined clades were assigned to within clade branches. All other support values, spanning from the outgroup to the clade branches, were recorded as backbone support values. Topology changes and conflicts were not accounted for. Based on this and on recommendations by studies investigating the impact of locus filtering for summary methods (Xi et al., 2016; Sayyari et al., 2017; Molloy and Warnow, 2018), we selected an average missingness threshold to filter the locus sets (Fig. 2c, "dataset selection avg. missingness"). The resulting dataset was subsequently used for comparative phylogenetic inference (Fig. 2d).

2.5.2 Locus filtering by length and dataset selection based on sub-dataset properties and phylogenetic patterns

In order to narrow down the suspected dataset bias in terms of fractional, non-random locus and/or taxon coverage, we used phylogenetic patterns to assess sub-datasets filtered by length. CA-ML inference of datasets exhibiting this type of bias can result in unsupported or overly high supported polytomies resolved as a terraced topology (Sanderson et al., 2010, 2011, 2015; Simmons et al., 2012; Dobrin et al., 2018). Dobrin et al. (2018) have reported numerous empirical multi-locus datasets to be impacted by this issue (e.g. Springer et al., 2012; Burleigh et al., 2015; Shi and Rabosky, 2015). Since we generated ML locus trees as input for species tree estimation with CB-SM, we assumed this terraced topology to also appear if the bias of the underlying data was strong. Besides, Hosner et al. (2016) and Sayyari

et al. (2017) found that a high proportion of fragmentary data (biased incongruence of locus trees) can lead to a sharp drop of the resulting BS support values for CB-SM inference.

In addition to the length interval sub-datasets of the first filtering ("int_min-250" – "int_551-max"), we filtered the loci requiring an increasing, cumulative maximum length (Fig. 2c, "locus filtering", Supplementary Table S7). The eight maximum locus length sub-datasets were generated starting at a threshold of 250nt ("max_250", all loci up to 250nt length were included) increasing by 50nt increments up to the maximum locus length. Each sub-dataset was subjected to phylogenetic inference using CA-ML and CB-SM. The sub-dataset properties and resulting BS support values were recorded as described in 2.5.1.

While bootstrapping across a concatenated matrix almost automatically increases the resulting support values with increasing matrix size (Kubatko and Degnan, 2007; Liu et al., 2015; Minh et al., 2020a), the multi-locus bootstrapping used with CB-SM employs a 2-stage system that accounts for variations among loci by resampling during BS calculation (Seo, 2008) and thus reacts very sensitive to fragmentary data (Xi et al., 2015, 2016; Hosner et al., 2016; Sayyari et al., 2017). We expected the BS support values to collapse as soon as the ratio of biased to unbiased data (respecting a non-randomly distributed partial taxon coverage) became too high. For CA-ML, we expected a similar but less sensitive pattern, in particular for the sub-datasets of an increasing maximum locus length.

For the evaluation of a terrace-like topology pattern, the number of samples resolved on terraced branches was recorded. We defined that a terraced branch must either -originate from a dichotomous branch of the tree's backbone, - the clade's backbone containing that sample, - or must follow an individual branch within a clade, - but must not be included within a dichotomous constellation. For instance, phylogenetic inference of the "raw" dataset using CA-ML, CB-SM and SVD resulted in two, five and three terraced branches for clade 5, respectively (Supplementary Figure S2). The SVD tree contained another terraced branch in

clade 4, but the CA-ML and CB-SM trees did not. By increasing the maximum locus length required, we expected the topology to switch from a terraced to a dichotomous tree pattern once the biased area has been passed or compensated (and vice versa). CB-SM was expected to react more sensitive than CA-ML due to the reduced amount of data, with individual gene trees as input (Xu and Yang, 2016). Therefore, the terraced pattern was assumed to be over-expressed once the amount of data became too small (in particular for the length interval sub-datasets), and likewise a larger portion of unbiased data would be needed for compensation (for the maximum length sub-datasets).

The dataset, which was intended to be a reasonable compromise for both methods, had to meet the following criteria: 1) relatively low average missingness, 2) relatively high ratio of PIS to SNPs, 3) relatively high BS support values for all tree sections, 4) relatively low number of samples resolved on terraced branches, 5) and had to avoid over- and under-represented assembly regions. The selected dataset was used for comparative phylogenetic inference (Fig. 2d).

2.5.3 Generating 'short' loci by locus truncation

The loci of the *ipyrad* "raw" assembly were truncated to one third of their original length to compare potential performance differences of the here generated loci to a RAD dataset obtained by assembly of 100nt PE reads. These shorter loci were intended to show less sequence variation and thus negatively affect phylogenetic inference. The truncated loci were re-arranged based on the selected datasets of the locus filtering (Table 1, Fig. 2c, "locus truncation").

2.6 Phylogenetic inference

We have chosen three commonly used approaches for phylogenetic inference of the generated main- and sub-datasets (Table 1, S6 and S7). CA-ML and CB-SM were used for inference during locus filtering. For the comparative phylogenetic inference, we additionally used SVDquartets as third inference approach. We decided not to test a full-coalescent method that uses co-estimation of locus trees and species trees such as implemented in BEST (Liu, 2008) or BEAST 2 (Bouckaert et al., 2014) because computation time and capacities required increase sharply with the number of loci and samples. Thus, full-coalescent methods are currently not practical for large-scale datasets with thousands of loci (e.g. Bayzid and Warnow, 2013; McCormack et al., 2013a; Zimmermann et al., 2014).

2.6.1 Phylogenetic inference with RAxML (CA-ML)

We used RAxML v8.2.12 (Stamatakis, 2014) to infer maximum likelihood phylogenies using GTRGAMMA as substitution model, 20 runs for BestML and 1,000 bootstrap replicates to assess statistical support of relationships. We used the unfiltered *ipyrad* supermatrix for inference of the "raw" assembly. For all other datasets, we concatenated individual loci to a supermatrix using FASconCAT v1.11 (Kück and Meusemann, 2010).

2.6.2 Species tree inference with ASTRAL-III (CB-SM)

ASTRAL-III v5.7.4 (Zhang et al., 2018) estimates species relationships based on gene/locus trees. To generate these locus trees, we used RAxML v8.2.12 (Stamatakis, 2014) under the GTRGAMMA model with 20 runs for BestML and 1,000 bootstrap replicates. ASTRAL was run in default mode using unrooted locus trees. We used multilocus bootstrapping (Seo, 2008) to compute branch support for the estimated species trees.

2.6.3 SVDquartets analysis (SVD)

SVDquartets (Chifman and Kubatko, 2014) is a quartet-based algorithm to compute species trees from SNP datasets. We used FASconCAT-G (Kück and Longo, 2014) to extract and concatenate the 25,320 parsimony informative characters (polymorphisms that are shared by at least two samples, PICs) of the 3,818 loci constituting the "raw" assembly. To meet the requirement for linkage of the dataset (sites must be unlinked), we randomly selected a single PIC of each informative locus for each dataset (Table 1, "unlinked PICs"). Analyses were run in SVDquartets as implemented in PAUP*4.0a168 (Swofford, 2003) with 1,000 bootstrap replicates under the multilocus bootstrap (Seo, 2008). The scripts for generating PIC datasets are available at GitHub (https://github.com/philipphuehn/RADseq-locus-filtering).

2.6.4 IQ-TREE analysis

We used IQ-TREE v2.1.2 (Minh et al., 2020a, b) to calculate the gene (gCF) and site concordance factors (sCF) of the resulting phylogenies, which give the percentage of decisive locus trees and alignment sites containing or supporting a specific branch in a given reference tree, respectively. Locus trees obtained with RAxML were used for gCF calculation. For sCF calculation, 1000 quartets were used to obtain stable estimations. To assess the resulting phylogenies with respect to a potential influence of biased data, we put the resulting topologies and BS support values in context with the gCF and sCF values and value differences. In general, both concordance factors are expected to be similar if the phylogenetic signal is only impacted by discordant signal, e.g. due to ILS (Minh et al., 2020a, b). If other processes affect the dataset, such as limited information or a data bias, the gCF values can be a lot lower than the sCF values, resulting in large factor value differences. A large proportion of conflicting signal or a significant variation of sites in the dataset can lead to a completely random resolution, which is indicated by sCF values ~33%. The reasons are either true

phylogenetic signal caused by ILS or biased signal caused by uneven coverage. Distinct factor value differences of alternative topologies may indicate non-phylogenetic signal.

3. Results

3.1 Final library and MiSeq output

The fragment distribution of the final library ranged from ca. 370-770nt. The majority of fragments outside the target range were successfully removed (Appendix 1, Fig. A1.4, A 1.5). The MiSeq runs generated a total of 6,870,208 paired raw reads for the 29 samples (Table S4, "samples"). Sequence quality decreased with increasing read length (Table S4, "run I-III"). The quality of the R2 reads started to decline below a Phred quality score of 20 from ca 260nt read length (Table S4, "mean quality scores"). The number of reads per sample ranged from 98,754 for *A. laxum* var. *latipetalum* Bañares & M.Marrero to 587,377 for *M. icterica* BG Bonn with an average of 236,903 reads per sample. Demultiplexed raw data is available at the NCBI Sequence Read Archive in BioProject PRJNA642981.

3.2 ISC and BSC threshold selection

In general, the plots of the selected metrics showed the expected trends and met the requirements (Fig. 3 and S1.B and S1.C). For the ISC metrics, however, the indicators were not as distinct as expected. The transition zones of the metrics were averaged to consensus CTs for the diploid and tetraploid samples, respectively (Supplementary Table S8).

For the ISC of diploid samples (Fig 3a and S1.B, "ISC 2n"), the onset of the undermerging area was initiated by an abrupt increase in the number of clusters at CT 0.95, which was indicated by a compression of the third quartile (Q3) for the CTs 0.93 and 0.94 and a simultaneous increasing slope intensity in the scatter plots (Fig. 3a and S1.B, "clusters total", transition zone: 0.93-0.94). Allelic variation was highest in the transition zone of 0.92-

580 0.95 and started to decrease strongly with increasing sample coverage (Fig. 3a and S1B,
581 "heterozygosity"). The peak CT for heterozygosity was 0.92 (transition zone: 0.92-0.95)
582 while the paralog peak was 0.88 (transition zone: 0.88-0.95). These maxima were preceded by
583 irregular jumps of adjacent medians and an intensity change of the slopes (Fig. S1.B). This
584 area was enclosed by the transition zone of the average read depth per cluster trend, which
585 was indicated by an increasing Q3 compression and a steady slope shift (Fig. 3a, Fig. S1.B,
586 "avg. depth total", transition zone: 0.92-0.95). The CTs within the described transition zones
587 were averaged to a consensus CT of 0.93 (Table S8, "ISC consensus CT").

588 For the ISC of tetraploid samples (Fig. 3b and S1.C, "ISC 4n"), undermerging was
589 initiated by a Q3 compression within the transition zone of the number of clusters and
590 increased in slope from CT 0.94 on (Fig. 3b and S1C, "clusters total", transition zone: 0.92-
591 0.93), while allelic variation also started to decline steeply with increasing CTs (Fig. 3b and
592 S1.C, "heterozygosity", peak at 0.94, transition zone: 0.89-0.94). The transition zone of the
593 average depth per cluster showed a steadily declining trend, a few slight median jumps and an
594 increasing Q2 compression (Fig. 3b and S1.C, "avg. depth total", transition zone: 0.89-0.92).
595 The transition zone of filtered paralogs showed a prominent median jump and a moderate
596 slope decline towards the undermerging area (Fig. 3b and S1.C, "filtered by maxH", peak at
597 0.90, transition zone: 0.90-0.92). The averaged consensus CT was 0.91 (Table S8, "ISC
598 consensus CT").

599 The scatter plots of the ISC metrics showed that some samples can have a larger effect
600 on the overall trend of a metric than others. For instance, the sample "A_tort_RIII_A36_J49"
601 (*A. tortuosum* subsp. *tortuosum*) showed one of the lowest average cluster depths ("avg. depth
602 total") while a high number of clusters ("clusters total") was found (Fig. S1.B). It also showed
603 the highest amount of filtered paralogs ("filtered by maxH") and a two times higher
604 heterozygosity than the other diploid samples, although flow cytometry confirmed its diploid

status (Table S1). The tetraploids also showed some samples that were clearly different from the others (Figure S1.C).

For the BSC threshold selection (Fig. 3c), the undermerging area was indicated by the steady increase in retained loci while the sequence variation (VAR) started to decrease at CT 0.92. At this point, the missingness of the assembly matrix was still low before it increased abruptly starting at CT 0.92. According to McCartney-Melstad et al. (2019) and Mastretta-Yanes et al., (2015), a suitable CT is right before the decrease in sequence variation and the steep increase in missingness while the sample coverage (retained loci) still increases, at CT 0.91. The hockey-stick signal was identified by the first positive swing of the "blade" following the NPL minimum (Fig. 3c, "new polymorphic loci", Paris et al., 2017). This upward swing was in the transition of the CTs 91/90 that corresponds to a CT of 0.91 (Table S8, "NPL") and thus supports the other requirements. We selected 0.91 as BSC threshold.

3.3 ipyrad assembly output

The average total read depth (avg_depth_total) for the diploid and tetraploid samples was 6.21 (± 2.17) at CT 0.93 and 5.55 (± 1.80) at CT 0.91, respectively (Supplementary Table S9, "ISC 2n", "ISC 4n"). After applying the min_depth threshold of 10 for clustering, the majority read depth (avg_depth_mj) rose to 40.24 (± 7.52) for the diploid and 39.22 (± 17.10) for the tetraploid samples. On average, 26,280 (± 11,873) clusters per individual were found for the diploids and 34,436 (± 15,023) clusters per sample for the tetraploids. The average count of consensus reads was 2,635 (±692) for the diploid and 2,633 (±645) for the tetraploid samples.

The unfiltered assembly using a BSC threshold of 0.91 comprised 3,818 loci and 71,691 variable sites (Table 1, Fig. 2, "raw" assembly). Of these variable sites, 36,413 were unique SNPs and 35,278 were PIS. 92 loci showed no variation and 581 loci contained no PIS. The dataset included 69.79% missingness, on average 10 unique SNPs and 9 PIS per locus. The

retained loci had an average length of 376nt (± 93) with a maximum locus length of 618nt (including uncalled bases and gaps). The majority of retained loci ranged in length from 250 to 550nt (Table S9, "locus coverage"). The assembly length range >500nt showed a prominent gap at ca. 540-580nt, after which a denser region with some samples of comparatively high coverage followed, at ca 590nt. Locus coverage per sample was fairly heterogeneous with an average of 1,242 (± 385) and ranged from a minimum of 640 loci for *A. laxum* A29_J41 to a maximum of 2,092 loci for *A. roseum* A01_J02 (Table S9, "sample coverage"). The two outgroup samples contained 127 (*M. icterica* M30_N36) and 155 loci (*M. icterica* BG Bonn) in the final assembly. The BLAST results showed that our dataset contained 21 loci (118 SNPs and 66 PIS) with identities of 78.5–100% with the reference plastomes. After removing non-parsimony-informative loci and cp loci, the dataset contained 3,225 loci with an average of 67.69% missing data. Each locus contained on average 10 SNPs and 11 PIS and had an average length of 379nt (± 93) (Table 1, "cleansed", Fig. 2c, "cp loci + 0-PIS loci removal").

3.4 Initial inference of the raw dataset and clade definition

Phylogenetic inference of the *ipyrad* "raw" assembly resulted in incongruent topologies (Table 2, Fig. S2). CA-ML (Fig. S2.A) and CB-SM (Fig. S2.B) yielded unsupported backbones, while the SVD reconstruction was fully supported (Fig. S2.C). All trees showed five well supported main clades: clade 1 comprised *A. laxum*, *A. pachycaulon* subsp. *parviflorum* and *A. palmense*, clade 2 included two subspecies of *A. pachycaulon,* subsp. *immaculatum* and subsp. *pachycaulon*, clade 3 was formed by three species from Madeira (*A. villosum*, *A. dumosum* and *A. divaricatum*), clade 4 comprised both subspecies of *A. tortuosum* and clade 5 comprised all remaining taxa (*A. roseum*, *A. punctatum*, *A. bituminosum*, *A. porphyrogenetos*, *A. brevipetalum*, *A. bollei* and *A. parlatorei*) as well as two subspecies of *A. pachycaulon,* i.e., *A. pachycaulon* subsp. *praetermissum* and subsp.

gonzalezhernandezii. Relationships among clades was not resolved due to a lack of reliable BS support among reconstructions.

3.5 Locus filtering

The 3,225 loci of the "cleansed" dataset (Table 1, Fig. 2c) were first filtered respecting the locus coverage (minimum number of samples required), the locus variability (VAR/locus length/number of samples) and locus length intervals by 50nt steps. The properties of the resulting sub-datasets were recorded and phylogenies were inferred using CB-SM (see 3.5.1, Table S6, Supplementary Figure S3, all tree files available at Mendeley, doi: 10.17632/yb6fd93dbw.1). For the second locus filtering, in addition to the length interval sub-datasets, the loci were filtered requiring an increasing, cumulative maximum length ("max length") and subjected to phylogenetic inference using CA-ML and CB-SM (see 3.5.2, Table S7, Supplementary Figure S4, all tree files available at Mendeley, doi: 10.17632/yb6fd93dbw.1).

3.5.1 Locus filtering by coverage, variability, length intervals and dataset selection based on average missingness

We created six "min samples" sub-datasets by increments of four (Fig. 4a, Table S6, Fig. S3). The locus count and sequence variation (total) decreased as the number of samples increased (Fig. S3.A1 and S3.A4). The average number of SNPs per locus remained nearly constant across datasets, whereas the number of PIS per locus increased proportionately with VAR/locus until the "min_samples_16" dataset and then remained constant when increasing the parameter (Fig. S3.A4 and S3.B1). As expected, missingness declined with increasing number of samples (Fig. S3.B1 and S3.C1). The average locus length was constant across the datasets (Fig. S3.B1 and S3.C4). The branch support values of the CB-SM phylogenies showed a steady, slightly decreasing pattern across the datasets (Fig. S3.D1 and S3.D2). The backbone and within clade support values were around 80 and dropped by ca ten points with

680 the “min_samples_24 dataset”. The average clade branch support was close to 100 in all
681 datasets.

682 Seven sub-datasets were filtered for the “min var” parameter (Fig. 4b, Table S6, Fig.
683 S3). The number of loci and sequence variation (total) decreased with increasing minimum
684 variability (Fig. S3.A2 and S3.A5). In terms of the sequence variation (VAR) total and per
685 locus, the ratio of SNPs to PIS shifted towards a higher SNPs proportion with increasing
686 required minimum variability (Fig. S3.A5 and S3.B2) and missingness increased as well (Fig.
687 S3.B2 and S3.C2). The average locus length decreased slightly with increasing variability
688 required, with the "min_var_300" sub-dataset showing a clear shift towards shorter loci (Fig.
689 S3.B5 and S3.C5). The BS support values showed a decreasing trend (Fig. S3.D2). The tree
690 topologies received varying support across the sub-datasets. The backbone branches were
691 supported highest for the “min_var_075” and “min_var_100” datasets, while the clade and
692 within clade branches had highest support values in the “min_var_001, 025, 050” datasets.
693 The average branch support decreased with increasing missingness (Fig. S3.D5).

694 The properties and resulting support values of the eight length interval datasets
695 showed irregular trends (Fig. 4c, Table S6, Fig. S3). The amount of loci and sequence
696 variation total (excluding the first sub-dataset containing only 72 loci) dropped from the
697 highest value at “int_251-300” to the adjacent dataset, then rose and declined moderately until
698 the next sharp decline from “int_451-500” to “int_501-550” (Fig. S3.A3 and S3.A6). The
699 average sequence variation per locus was rising with increasing locus length. The proportions
700 of SNPs and PIS in sequence variation (VAR) shifted towards a higher proportion of
701 parsimony-uninformative sequence variation for the datasets “int_min-250” and “int_551-
702 max”, respectively (Fig. S3.B3). The missingness had a slightly convex trend with maxima
703 for the flanking datasets (Fig. S3.B6 and S3.C3). The steadily increasing trend of the locus
704 length showed unexpected averages for the two datasets containing the longest loci (Table S6,

Fig. S3.B6 and S3.C6), matching the uneven locus length distribution of the "raw" assembly (Table S9, "locus length distribution" and "locus coverage"). The resulting branch support values showed contrasting patterns (Fig. S3.D3 and S3.D6). The overall trend was shaped concavely. The backbone support initially increased to a maximum at "int_401-450" and then decreased with increasing locus length. The average clade support values were highest at "int_251-300", "int_351-400" and "int_451-500". The within clade branches were supported highest by the "int_351-400" sub-dataset, embedded in a descending trend towards the dataset edges.

Regarding the "min_samples" and the "min_var" datasets, the results were as expected and consistent with findings of previous studies (e.g. Chen et al., 2015; Huang and Knowles, 2016; Eaton et al., 2017; Molloy and Warnow, 2018,). For both parameters, the overall support decreased with increasing requirements, likely due to the simultaneous decline in number of loci and sequence variation. The irregular trends of the locus length interval datasets provided useful clues for subsequent dataset selection and further filtering (see 3.5.2). The trends observed here, together with the declining read quality (Table S4), the heterogeneous coverage of samples and loci, and the irregular assembly coverage respecting the over- and under-represented locus length ranges from ca. 250-280nt and ca. 540-580nt (Table S9), fit the definition of so-called "biased missingness" (Xi et al, 2015, 2016; Hosner et al., 2016; Sayyari et al, 2017; Molloy and Warnow, 2018). To reduce this impact, we selected the average proportion of missingness (69.58% for the length interval datasets) as threshold and discarded all datasets above this cut-off. The retained "int_251-500" dataset (Table 1, "int_251-500") consisted of 2,788 loci, containing in total 56,448 (20.24 ±15.7 on average) VAR, 26,533 (9.51 ±8.66) SNPs, 29,915 (10.73 ±10.76) PIS, 66.66% missingness (9.67 samples/locus) and the average locus length was 360 (±70nt). The locus truncation to one third of the original length lead to a 2/3 reduction of sequence variation and locus length (Table 1, "int_251-500_short").

3.5.2 Locus filtering by length intervals and increasing maximum length and dataset selection based on data qualities and phylogenetic patterns

The conspicuous trends of the length interval datasets in terms of SNPs/PIS ratio and missingness/locus coverage relative to the resulting BS support values of the species tree sections motivated further filtering to narrow down the extent of potential biased missingness (Table S7 and Fig. S4).

For the locus length interval datasets, CA-ML showed the lowest and highest average BS support values for the “int_0-250” and “int_251-300” datasets, respectively (Fig. S4.C2 and S4.D1). The average branch support decreased steadily with increasing locus length. The three branch sections were irregularly supported by different sub-datasets. The highest count of terraced branches was found for both CA-ML and CB-SM for the "int_0-250" dataset (Fig. S4.D2). The second highest counts were recorded for the sub-datasets “int_501-550” and “int_551-max”, respectively. CA-ML resolved the fewest terraced branches for the “int_301-350” and “int_351-400” sub-datasets. The CB-SM trees showed the smallest counts for the “int_251-300” and “int_351-400” datasets, with the latter having the highest average BS support value (Fig. S4.D1 and S4.D3).

For the maximum length datasets, CA-ML showed the lowest sectional and total average BS support values for the first two sub-datasets (Fig. S4.C4 and S4.D2). Then, the BS support raised sharply for the “max_350” sub-dataset and increased steadily up to the maximum for the “max_500” sub-dataset. Beyond this point, there was no gain in branch support. The CB-SM branch support values were lowest for the “max_250” sub-dataset, increased slightly until the “max_350” sub-dataset, showed a strong gain for the “max_400” and a maximum value for the “max_450” sub-dataset (Fig. S4.C2 and S4.D2). Then, the average BS support decreased with increasing maximum locus length, in particular the backbone section lost support. CA-ML and CB-SM resolved the highest terraced branch count for the first sub-dataset (Fig. S4.D4). The number of terraced branches decreased to a

minimum of two for the CA-ML trees with increasing maximum length required. CB-SM resolved the fewest terraced branches for the "max_400" sub-dataset. With the addition of loci up to 500nt length ("max_500") the terraced branch count increased strongly and remained high up to the maximum locus length ("max_length").

For the final dataset selection, we classified all recorded locus properties of the sub-datasets and the phylogenetic patterns of the resulting trees into three categories, respectively (Fig. S4.E). The two extreme datasets of both assembly edges were either over- or under-represented (Table S9, "locus length distribution" and "locus coverage"). Those sub-datasets showed also a higher or almost equal ratio of SNPs to PIS relative to the average VAR per locus (Fig. 4, "int_datasets", Table S7, Fig. S4.A1-A6). The average missingness was highest for the filtering parameter edges and decreased towards the inner medium parameters (Fig. S4.B1-B4). The expected average locus lengths were met by the inner filtering parameters, while the values of the sub-datasets increasingly diverged towards the assembly edges (Fig. 4, "int_datasets", Table S7, Fig. S4.B5 and S4.B6). Both CA-ML and CB-SM showed the highest sectional and total BS support values for the inner filtered sub-datasets, with the highest gain for the "max_350" and "max_450" sub-datasets (Fig. S4.C1-C4 and S4.D1-D2). The BS support values of the backbone section profited most within this locus length range. Both approaches resolved the highest number of terraced branches for the filtering parameter edges (Fig. S4.D3-4). The terraced branch count decreased with increasing maximum locus length and increased again strongly beyond a locus length of 450nt for the CB-SM trees. With this locus length also the BS support values started decreasing steadily (Fig. S4.D2 and S4.D4). In summary, the locus properties and phylogenetic patterns associated with non-randomly distributed missingness or biased data were strongest at the filtering parameter edges, while the length ranges from 300 to 450nt appeared to be less affected (Fig. S4.E). The selected "int_301-450" dataset (Table 1) consisted of 1,599 loci of an average length of 373nt (±43nt), containing 15,673 SNPs (avg. 9.82), 17,808 PIS (avg. 11.24) and 65.56%

783 missingness. Truncation resulted in a 2/3 reduction of locus properties (Table 1, “int_301-
784 450_short”).

785 *3.6 Phylogenetic inference*

786 We used three datasets for comparative phylogenetic inference (Table 1, Fig. 2c and
787 2d). The 3,818 loci of the "raw" assembly were used for initial inference and clade definition
788 (see 3.4). We removed both cp and non-informative loci from this dataset. The retained 3,225
789 loci of the “cleansed” dataset were the input for the locus filtering approach (see 2.5 and 3.5).
790 The first locus filtering by coverage, variability and length intervals resulted in the “int_251-
791 500” dataset (see 2.5.1 and 3.5.1). The second locus filtering was intended to reduce the
792 presumed biased phylogenetic signal by using phylogenetic patterns relative to the underlying
793 sub-dataset qualities to detect impacted assembly areas (see 2.5.2 and 3.5.2). This approach
794 yielded the “int_301-450” dataset. The filtering steps reduced the number of loci by 58% and
795 the amount of PIS by 50% (Tab. 1, “raw” compared to “int_301-450”). Sequence variation
796 and locus coverage increased slightly while the average missingness decreased by 4%. Loci-
797 per-sample coverage decreased from an average of 1,166 to 549 loci while sample-per-locus
798 coverage became more homogenous (Table S9, “sample coverage”). Hence, we assumed the
799 "raw" assembly to contain the most, the "int_251-500" dataset to contain less, and the
800 "int_301-450" dataset to contain the least biased phylogenetic signal. Filtering parsimony
801 informative characters (unlinked PICs) resulted in three datasets for the SVD analyses (Tab.
802 1). The loci of the “raw” assembly were truncated to one third of their original length, re-
803 arranged respecting the locus filtering results and species relationships were inferred with
804 CA-ML and CB-SM to compare potential performance differences in terms of locus length
805 (Table 1, “short”, Fig. 2c and 2d).

806

807 *3.6.1 Comparative phylogenetic inference of the un-/filtered datasets*

808 For the "raw" datasets, CA-ML (Fig. S2.A) and CB-SM (Fig. S2.B) resolved
809 incongruent and weakly supported backbone topologies. The CA-ML tree showed an
810 unresolved relationship between the clades 2, 3 and 4. CB-SM inference resulted in an
811 unresolved relationship of clade 1 to clades 2, 3 and 4, with low support and low concordance
812 factor values. The SVD tree (Fig. S2.C) showed full support for a third topology. However,
813 the concordance factor values for the relationship of clade 1 to clade 5 were low. The within
814 clade topology differed among all reconstructions.

815 For the "int_251-500" dataset, CA-ML (Supplementary Figure S5.A) and CB-SM
816 inferences (Fig. S5.B) resolved congruent backbone topologies, however, for CB-SM the
817 relationships of clades 2+3+4 to clade 5 lacked support. The concordance factor values
818 increased compared to the "raw" dataset. The SVD tree (Fig. S5.C) showed a maximally
819 supported conflicting topology with low concordance factor values for the relationship of
820 clade 2 to clades 1+3+4. The within clade topology differed among all reconstructions.

821 For the "int_301-450" dataset, CA-ML (Supplementary Figure S6.A) and CB-SM
822 (Fig. S6.B) inference resulted in a well-supported, congruent backbone topology (Fig. 5).
823 Concordance factor values for the backbone and clade branches were similar. Again, the SVD
824 tree (Fig. S6.C) showed a maximally supported conflicting topology but low concordance
825 factor values for the relationship of clade 2 to clades 1+3+4.

826 *3.6.2 gCF and sCF values obtained with IQ-Tree*

827 Dataset reduction with respect to the exclusion of potentially biased assembly areas,
828 clearly showed an improvement regarding the concordance factor values and differences for
829 the CB-SM reconstructions (Tab. 2). The factor difference decreased for all within clade
830 branches and clade branches. The factor values of the clades 1, 2, 3, and 5 decreased stronger
831 compared to clade 4. The gCF value of the clade branches increased by more than 8%
832 compared to the unreduced dataset, while the sCF value decreased slightly. Interestingly, the

833 factor values of the backbone branches increased slightly while the difference increased
834 slightly as well.

835 Concordance factors of CA-ML inference showed a similar pattern compared to CB-
836 SM. Overall, the factor values increased with increasing dataset reduction. However, the
837 effect was less pronounced compared to CB-SM and clade 5 even showed an increased factor
838 difference. Notably, the effect of the factor differences for the clade branches was smaller
839 while for the backbone branches it was larger, compared to the CB-SM reconstruction.

840 In general, the factor effects of the SVD reconstructions were in strong contrast to CB-
841 SM and CA-ML. The SVD factor values were lower compared to CB-SM and CA-ML, and
842 the factor differences raised for the clade and the backbone branches. For the within ancestral
843 branches of clade 2+3 and all descendant relationships, the factor difference decreased
844 strongly.

845 In terms of the resulting BS support values, data reduction had the strongest effect on
846 the backbone branches with an increase in support by ~13% for CA-ML and ~16% for CB-
847 SM (Tab. 2). Still, the gCF and sCF values suggest alternative topologies for the relationship
848 of clades 2+3+4 to clade 5.

849 *3.6.3 Phylogenetic inference of the truncated locus datasets*

850 Inference of the truncated datasets using CA-ML (Supplementary Figure S7.A and
851 S7.B) and CB-SM (Fig. S7.C and S7.D) resulted in alternative topologies compared to the
852 full-length datasets, while also exhibiting distinctly lower concordance factor values and
853 larger factor differences (Supplementary Table S10) or insufficient BS support for the
854 backbone section. The BS support values decreased with decreasing locus length and the
855 decrease was strongest in the backbone branches. The concordance factor values were mostly

856 lower compared to the full-length datasets and the factor difference for the clade and

857 backbone branches increased clearly for all reconstructions.

4. DISCUSSION

Modification of several modules of the RADseq toolbox, inspired by GBS (Elshire et al., 2011) and ddRADseq (Peterson et al., 2012), has enabled a strong reduction of the number of targeted fragments. In addition, employing the maximum capacity for sequencing resulted in an extended locus length of up to 618nt. The CT selection approach enabled an informed selection of ISC/BSC thresholds for homology assessment of assembled loci. The locus filtering approach, based on properties known to affect phylogenetic inference, provided the opportunity to observe dataset-specific trends and identify potential adverse properties of the sub-datasets. Additional filtering using phylogenetic patterns for bias detection turned out to improve overall resolution, in particular for CB-SM inference. Besides these positive outcomes, there were also many challenges whose critical consideration led to suggestions for further improvements.

4.1 Lab workflow

Compared to other studies employing a RADseq approaches for sample preparation (e.g. Escudero et al., 2014; de Oca et al., 2017; Dillenberger and Kadereit, 2017; Hamon et al., 2017; Wagner et al., 2018; Gerschwitz-Eidt and Kadereit, 2019; Paetzold et al., 2019; Rancilhac et al., 2019; Hipp et al., 2020; Karbstein et al., 2020) we increased the fragment length range and thus the length of assembled loci clearly by shifting the size selection window and fully exploiting the sequencing range of 300nt PE. However, the raw reads varied strongly both in quantity and quality across the samples, which led to a loss of locus and sample coverage, in particular within the higher length range targeted (Supplementary Table S9). This biased distribution of phylogenetic information represented a substantial challenge to data evaluation.

Our lab workflow aims at long RAD loci and has been modified in three aspects: First, we included a specific size selection window ranging from 300–600nt for the resulting

fragments of the utilized REases BamHI and KpnI. Second, barcode and common adapters were designed for both REase motifs to sequence all generated fragment types in contrast to the classic ddRADseq approach (compare Peterson et al. 2012). Third, the lab protocol contained two size selection steps to ensure complete removal of fragments outside the target range.

4.1.1 Employed REases

The flexible RADseq toolbox allows the use of various REases of a wide range of qualities for complexity reduction (see also: Andrews et al., 2016; McKain et al., 2018; Parchman et al., 2018). Testing and comparing single and dual enzyme strategies with respect to the desired degree of reduction, or in particular a reduced fragment number and an extended length range, either *in silico* or by sequencing a trial library when there is no reference available, can certainly reduce mutation-based locus dropout and ease library prep and adapter design (see also: Lepais and Weir, 2014; Mora-Marquez et al., 2017; Rivera-Colón et al., 2021). Double-digest approaches, using two REases for digestion (e.g. Peterson et al., 2012), are more prone to restriction site mutation disruption than single-digest protocols (e.g. Elshire et al., 2011). Hence, they tend to yield fewer fragments than single-digest approaches which are therefore more easily sequenced to sufficient depth (Andrews et al., 2016; Harvey et al., 2016; Eaton et al., 2017; McKain et al., 2018). Using the *K. fedtschenkoi* genome for *in silico* double-digest using *BamHI* and *KpnI*, we calculated about 4,400 fragments (see 2.2) and received about 3,800 assembled loci (Table 1, "raw"). The difference of ca. 600 fragments may be due to the loss of loci in the assembly range above 500nt (Table S9). Compared to capturing approaches, which typically produce loci of up to thousands of base pairs in length (e.g., McCormack et al., 2013a; Nicholls et al., 2015) the herein obtained locus length of Ø 376nt and 618nt at most may seem short. Still, the resulting loci showed sufficient sequence variation per locus as input for species tree estimation using

CB-SM and were in line with approaches targeting similar length ranges (e.g. Hosner et al., 2016; Blom et al., 2017).

4.1.2 Adapter design

The design of adapters herein was based on the original GBS protocol to include and sequence all generated fragments (see Elshire et al., 2011). However, this approach proved not satisfactory. It did not account for potential chimera formation and index hopping (see also: Van der Valk et al., 2020) and the identical flow cell binding motifs meant a potential reduction in sequencing yield. While in general the sequencing output was not influenced, the second sequencing run, containing the majority of samples, yielded only 50% of the maximum sequencing output of the MiSeq v3 kit (Table S4, "run III"). In addition, the reads flanked by identical cut sites introduced a further step in data processing and locus assembly that could be avoided as the raw data had to be demultiplexed twice. Considering these hurdles, we recommend to design each adapter type for one cutsite motif only and to use an indexing approach that accounts for technical bias (e.g. MacConail et al., 2018; Bayona-Vásquez et al., 2019).

4.1.3 Size selection window and fragment/locus length distribution

The use of coalescent-based summary methods for phylogenetic inference requires a relatively high quality content of sequence variation per locus to reduce GTEE (Chou et al., 2015; Liu et al., 2015; Mirarab et al., 2016; Xu and Yang, 2016; Molloy and Warnow, 2018). Because the average amount of phylogenetic information in a neutrally evolving locus generally correlates with its length (Blom et al., 2016; Mirarab et al., 2016; Chou et al., 2016; Molloy and Warnow, 2018), we chose a size selection window of approximately 300-600nt (ca. 380-720nt segregation range including the adapter and primer length) to obtain longer fragments and thus more informative loci (Fig. 1, Appendix 1). The 2nd size selection using a ratio of 0.8 parts magnetic bead suspension to one part library suspension is particularly

important as it removes fragment artifacts from automated fragment segregation and PCR (Fig. 1f, Appendix 1). Compared to a library prepared with the same protocol but without final purification, the precision of the fragment length segregation was clearly improved (Appendix 1). The length distribution of the final assembly was overall in the range targeted by the lab protocol. However, the strong decline in sequencing quality of R2 reads (Table S4, "run I-III", "mean quality scores") has resulted in a large degree of missingness in the length range of 500-600nt of assembled loci (Table S9, "locus length distribution"). Moreover, the quality filtering thresholds were set quite strictly (Table S5; Eaton and Overcast, 2020). This prevents assembly of erroneous sequences by discarding reads below a specified threshold for base and overall quality. In our dataset this applied especially to the R2 reads, starting at ca 260nt. Thus, a lot of information was lost by excluding high quality partners of low quality mates. Tan et al. (2019) found that declining base quality and higher error rates of fragments above 500nt are a general issue with multiple Illumina sequencing platforms and kits.

The descriptive analysis of the filtered sub-datasets showed that phylogenetic information across the length intervals provided varying support for different sections of the resulting species trees (see 2.5.2 and 3.5.2, Fig. 4c, Fig. S4, "length interval datasets"). Maximum support for all sections was covered by a locus length range of 300-450nt. Considering this and the decreasing quality of R2 reads, we recommend a size selection window of 300-500nt (ca. 380-620nt segregation range including the adapter and primer length). This might avoid locus loss due to the decreasing sequencing quality of the R2 reads and thereby achieve a more uniform assembly and evenly distributed phylogenetic information. However, other focal groups than *Aichryson* might require longer loci, as the retained variation per locus depends on the taxonomic level of interest and is very group specific.

4.2 Data analysis

Assembly and analysis of RADseq data is often challenged by various factors depending on the selected library prep and bioinformatics approach, and, of course, the study group itself. The *Aichryson* data shown here united just about every conceivable challenge known to RADseq data. The samples had varying DNA qualities and were sequenced in three different libraries. The output of the three sequencing runs differed in terms of quantity and quality. The R2 reads showed an unevenly distributed drop in quality starting at about 260nt sequencing length (Table S4). And it turned out that this dataset had not only a high proportion of missing data, but also of biased missingness across the assembly length range, impacting sample and locus coverage (Table S9). Despite these unfavorable circumstances, or maybe because of them, the detailed analyses (Fig. 2), including a CT selection and a locus filtering approach, provided detailed insights into the data properties and their impact on phylogenetic inference.

4.2.1 CT selection approach

Clustering threshold selection approaches aim at determining balanced CTs to establish homology while avoiding clustering of paralogous RADseq loci (e.g., Ilut et al., 2014; Mastretta-Yanes et al., 2015; McKinney et al., 2017; Paris et al., 2017; McCartney-Melstad et al., 2019). For this purpose, assembly metrics are compared across a range of CTs to identify values that meet specified requirements. Application of such methods is becoming increasingly popular (e.g. Herrera and Shank, 2016; Razkin et al., 2016; Paetzold et al., 2019; Rancilhac et al., 2019; Karbstein et al., 2020; Wagner et al., 2020) to ensure the assembly of homologous loci (Shafer et al., 2017; Springer and Gatesy, 2018; McCartney-Melstad et al., 2019; Fernández et al., 2020; Simion et al., 2020). Following these previously proposed criteris, we were able to identify areas that met the requirements in terms of 1) the onset of the undermerging area, in which true orthologs are separated into paralogs (McCartney-Melstad

et al., 2019), 2) an area of high heterozygosity with decreased clustering of paralogs (Ilut et al., 2014), 3) a maximized sequence variation count while missingness is minimized (Mastretta-Yanes et al., 2015), and 4) an increasing number of new polymorphic loci (NPL) indicated by the hockey stick signal (Paris et al., 2017). This procedure resulted in an assembly comprising 3,818 loci, of which ~84% contained parsimony informative sites (Table 1). The loci showed on average ~19-21 variable sites, of which ~9-11 were parsimony informative. Since these loci were found to be useful for CB-SM inference, we consider the here selected metrics and CT selection approaches in general as promising tools for an informed selection of thresholds during *de novo* assembly. Still, there are some issues that need to be considered: 1) The results shown herein and assumptions arising from them provide more empirical evidence on previous studies, however, are highly specific to our study group and do not constitute proof in general. Hence, simulation studies with known characteristics and focusing on each of these aspects are urgently required. 2) We selected only a few out of many more possible metrics that can be utilized to evaluate dataset-specific trends, such as the pairwise data missingness and genetic dissimilarity (McCartney-Melstad et al., 2019), the proportion of heterozygous loci in a sample and allelic ratios at each locus (McKinney et al., 2017) or the fraction of sequence variation shared by specific proportions of all individuals (Paris et al., 2017). 3) The selected CTs for ISC and BSC are an adequate representation of a majority of loci but one CT cannot appropriately characterize the entire sequence divergence within and across samples. Various causes of sequence divergence among genomic regions (e.g., coding or non-coding regions, thus degree of sequence conservation, and biological processes such as hybridization, horizontal gene-transfer and ILS) lead to a normalization within a range of suitable CTs, which we here referred to as the "transition zone". 4) Polyploid loci composed of greater allele numbers can show greater heterozygosity than loci composed of lower number of alleles presumably containing less sequence variation across orthologous alleles (Hirsch and Buell, 2013; Karbstein et al., 2021),

and thus require different CTs for accurate clustering. Hence, merging of ISC samples of varying ploidy for BSC across all taxa leads to a clustering bias. 5) The resulting data, whether used for metric evaluation or inferences of population structure or species relationships, are heavily impacted by all other parameters chosen, depend on numerous properties of the study system (e.g.: taxonomic level, genomic variation, utilized lab protocols, quality and quantity of data) and will affect downstream analysis (e.g. Huang and Knowles 2016; Eaton et al., 2017; Shafer et al., 2017; Crotti et al., 2019; McCartney-Melstad et al., 2019). 6) Metric trends can be affected by heterogeneous read quality and quantity, as well as biological factors, such as genome size or repetitive regions. This presumably leads to different metric trends of individual samples, as seen in the scatter plots for the ISC threshold selection (paragraph 3.2, Supplementary Figure S1). As a consequence, the selection of potential CTs gets less precise. This problem may be improved by re-splitting samples into groups that show similar trend intensities and using specific CTs for each group. Simulation studies focusing on potential impacts of heterogeneous sample qualities on the CT selection and the resulting assembly are required. Nevertheless, we consider a thorough evaluation of assembly metrics, as shown in this and other studies (e.g. Paris et al., 2017; Paetzold et al., 2019; Rancilhac et al., 2019; McCartney-Melstad et al., 2019; Karbstein et al., 2020; Wagner et al., 2020), to be an improvement over simply using default settings.

4.2.2 Locus filtering

The impact of filtering loci regarding specific properties, such as length, sequence variation or missingness, prior to phylogenetic inference has been investigated by numerous studies (e.g. Chou et al., 2015; Liu et al., 2015; Xi et al., 2015, 2016; Hosner et al., 2016; Mirarab et al., 2016; Huang and Knowles 2016; Sayyari et al., 2017; Molloy and Warnow, 2018). We confirm general trends previously observed regarding locus coverage and sequence variation (see 2.5.1 and 3.5.1, Table S6, Fig. S3). As the minimum requirements increased,

the number of loci and sequence variation decreased (Huang and Knowles, 2016; Eaton et al., 2017). This information loss resulted in sharply decreasing BS support values of the resulting species tree estimates. This is likely a result of higher locus dropout in more rapidly evolving loci (for the "min var" datasets). The more conserved loci are less variable but also less prone to mutation-induced cut-site disruption and thus show a higher sample coverage (for the "min samples" datasets). An interesting point is that the two datasets with the highest minimum variability required (Table S6, "min_var_200" and "min_var_300") also showed a trend toward biased locus lengths. In addition, these loci contained on average more missing data and a higher portion of variable sites was parsimony un-informative. The negative impact of this constellation of locus properties on the accuracy of species tree estimation has been demonstrated by Xi et al. (2015), Hosner et al. (2016) and Lee et al. (2018). This constellation was also evident for the length interval datasets containing the shortest and longest loci at the assembly edges (Table S6 and S7, Fig. S3 and S4). For these assembly regions, we assume that the declining sequencing quality of R2 reads led to biased sample and locus coverage, which was reflected by the prominent gap between 500-600nt as well as the high number of loci in the 250-300nt length range of the assembly (Table S9). This kind of data bias causes high GTEE and artificial phylogenetic conflicts among taxa and clades, which negatively affects the species tree estimation performance (Sanderson et al., 2010, 2011, 2015; Simmons et al., 2012; Hosner et al., 2016; Xi et al., 2016; Sayyari et al., 2017; Dobrin et al., 2018).

To reduce this effect, we first chose a controversial approach and filtered the loci based on average missingness, which resulted in the "int_251-500" dataset. Locus filtering based on missingness is generally not recommended because it can lead to a significant loss of information and thus to a performance decline of phylogenetic inference (Huang and Knowles 2016; Eaton et al., 2017; Molloy and Warnow, 2018; Crotti et al., 2019). However, it can lead to an improvement in estimation accuracy if the extent of biased, non-randomly distributed phylogenetic signal is also reduced (Xi et al., 2015, 2016; Sayyari et al., 2017;

Molloy and Warnow, 2018). Although this first filtering and dataset selection resulted in a slight improvement of the data quality and the resulting BS support and concordance factor values, it did not yield the required data quality for a successful CB-SM inference. Simply choosing the average missingness as a cutoff value may improve the quality of loci containing evenly distributed phylogenetic information, but not if the bias is unevenly distributed across the assembly.

To further reduce the extent of the biased assembly area, we binned the loci based on length, inferred CA-ML and CB-SM phylogenies for each sub-dataset and put resulting phylogenetic patterns in relation to sub-dataset properties to detect biased locus length ranges (see 2.5.2 and 3.5.2, Table S7, Fig. S4). This approach turned out beneficial with regard to the selection of less biased assembly areas, suitable for CB-SM inference. The typical responses of BS support values and reconstruction of terraced branches confirmed the assembly's edge regions as particularly biased. In these locus length regions of the assembly, either the BS support values collapsed or the number of terraced branches of the resulting topology was high. Consequently, we selected the remaining, presumably less biased, assembly range of 301-450nt length served as third dataset for comparative phylogenetic inference. While this second filtering and dataset selection procedure represented a drastic reduction of overall data quantity, it also increased data quality as indicated by the average sequence variation per locus, locus coverage/missingness and sample coverage (Table 1, Table S9).

The second filtering approach used here to examine the influence of locus properties on the resulting phylogenetic reconstructions resulted in a dataset favorable for CB-SM inference. However, the process was quite tedious, and at times somewhat crude, which indicates a number of opportunities for further refinement in the future. 1) Loci of certain properties within the excluded assembly ranges are likely to be also well suited for CB-SM inference. We filtered the loci by their relative sequence variation including SNPs and PIS

(see 2.5.1). However, the notable PIS/SNPs ratio along with the average locus coverage evident in the locus length filtering (Fig. S3 and S4) may be a clue to filter loci by information quality (Xi et al., 2015; Hosner et al., 2016; Lee et al., 2018). 2) The bin sizes chosen for filtering locus properties might be smaller to enable a more accurate detection of potential trend changes respecting phylogenetic outcomes. 3) We calculated only one reconstruction per inference approach for each sub-dataset. Multiple replicates may be generated to identify and statistically assess potential variations. 4) We found overall matching trends of locus properties relative to the resulting phylogenetic patterns of CA-ML and CB-SM used for bias detection. Considering the presumably strongly biased signal scattered across taxa, the relative influence of technical errors and true biological conditions (e.g. ILS) remain difficult to assess. 5) Instead of multi-locus bootstrapping (Seo, 2008), the branch support might be assessed using Local Posterior Probability, which was shown to perform more accurate on locus trees with relatively high error (Sayyari and Mirarab, 2016) or quartet based methods to identify non-informativeness (Pease et al., 2018). 6) Counting the terrace-like branches in the resulting trees helped to identify biased assembly areas but did not provide insight into the actual underlying conflicts among taxa and clades. Besides, terraced branches can also represent the true topology (Sanderson et al., 2011). To account for artificial conflicts in the data, terrace-aware phylogenetic inference tools can be used (Sanderson et al., 2011, 2015; Chernomor et al., 2016; Dobrin et al., 2018). 7) Further approaches may be tested comparatively to allow for a more accurate data quality assessment, such as filtering for fragmentary data to achieve uniform taxon coverage (Xi et al., 2016; Sayyari et al., 2017) or subsampling specific loci to establish congruence across the dataset (Chen et al., 2015; Simmons et al., 2016). For future projects, an automated pipeline that filters loci based on multiple criteria, records the properties of these bins, and evaluates the resulting phylogenetic patterns, thus simplifying the tedious filtering process, would be of great value.

4.3 Phylogenetic inference

Previous attempts at resolving phylogenetic relationships in *Aichryson* were mainly hampered by lack of variability in the employed regions (Mort et al., 2002; Fairfield et al., 2004 which failed to resolve relationships at shallow taxonomic levels (e.g., Miller et al., 2003; Abeysinghe et al., 2009; Duan et al., 2015). The application of a modified RADseq approach together with detailed data processing, analysis of filtered sub-datasets and comparative phylogenetic inference resulted in the first well-supported phylogeny for *Aichryson*. Moreover, we gained further insight into the performance of the tested inference methods with respect to underlying data properties.

4.3.1 General trends of the CA-ML and CB-SM inference during locus filtering

During locus filtering, we initially filtered the loci by variability, locus coverage and length intervals (see 2.5.1 and 3.5.1). Contrary to our expectation, we were not able to reconstruct a well-supported CB-SM phylogeny using this approach. Instead, we found that the BS support values of the three species tree sections responded differently to the underlying locus length interval datasets (Fig. 4, Table S6, Fig. S3). The related locus properties in terms of sequence variation and missingness, as well as the distribution of data across the assembly, loci, and samples (Table S9), indicated a data bias (Sanderson et al., 2010; Hosner et al., 2016; Xi et al., 2016; Sayyari et al., 2017; Lee et al., 2018; Molloy and Warnow, 2018).

Subsequently, we used phylogenetic patterns yielded by CA-ML and CB-SM inference of locus length sub-datasets to detect potentially biased assembly areas (see 2.5.2 and 3.5.2, Table S7, Fig. S4). CB-SM resolved more terraced branches than CA-ML across the tested sub-datasets, in particular when the datasets were small (Xi et al., 2016; Fig. S4, “length interval” datasets). This is likely due to the information loss inherent to the method, using only summary statistics of the inferred gene trees as input for species tree estimation (Xu and Yang, 2016). Along with this come the clearly lower resulting support values of the multi-locus bootstrapping

(Seo, 2008) when applied to fragmentary data (Xi et al., 2015, 2016; Hosner et al., 2016; Sayyari et al., 2017). The overall higher and steadily increasing BS support values with increasing dataset size confirm prior observations regarding CA-ML inference (Kubatko and Degnan, 2007; Liu et al., 2015; Minh et al., 2020a). CA-ML inference of the length sub-datasets seemed less sensitive or more robust to data bias (Xi et al., 2016; Molloy and Warnow, 2018). Still, bootstrapping over the concatenated matrix showed quite similar trends compared to the multi-locus bootstrapping employed with CB-SM.

4.3.2 Comparative phylogenetic inference of the un-/filtered datasets

The filtering steps meant a maximum reduction of 58% for the number of loci and 50% for the number of PIS, while the average sequence variation and coverage per locus raised, average missingness declined and sample coverage became more evenly distributed (Tab. 1, "raw" compared to "int_301-450", Table S9, "sample coverage").

For CA-ML and CB-SM, the exclusion of presumably biased assembly areas, resulted in increasing statistical support while the concordance factor value differences decreased (Tab. 2, Table S10, Fig. S2, S5 and S6). These trends were stronger for the CB-SM inferences. The concordance factor values and differences of the within clade branches benefited slightly while those of the clade branches benefited most from reduction. This was accompanied by improved factor values and differences of the backbone branches. We suggest that the overall higher locus coverage and the more evenly distributed information across taxa (sample coverage) of the retained assembly area caused less artificial conflicts among clades and thus favored resolution and support of the backbone section (Sanderson et al., 2010, 2011; Xi et al., 2015, 2016; Hosner et al., 2016; Sayyari et al., 2017; Dobrin et al., 2018; Molloy and Warnow, 2018; Minh et al., 2020a, b). This increasing statistical support coincides with an increase in the number of terraced branches. For instance, the CA-ML and CB-SM inferences of the "raw" dataset reconstructed a dichotomous topology for the taxa of clade 4, but there was insufficient

statistical support for the backbone sections (Fig. S2). The backbone topology of the strongly reduced "int_301-450" dataset was well supported, but in exchange the taxa of clade 4 were reconstructed on terraced branches (Fig. 5 and S6).

Phylogenetic inference of the datasets using SVD showed some contradictions. The lower factor values of the backbone branches for the alternative topologies and compared to the CA-ML and CB-SM inferences (Fig. S2, S5 and S6), increasing concordance factor value differences with increasing extent of reduction (Table 2), as well as the consistent maximum BS support values, suggest a random resolution due to limited and unevenly distributed information (Long and Kubatko, 2018; Minh et al., 2020a, b). This is certainly in part due to the selection of individual PICs per locus, which we performed to meet the methods requirements in terms of linkage (Bryant et al., 2012; Chiffman and Kubatko 2014; Xu and Yang, 2016). In addition, studies comparing the performance of inference methods under challenging data conditions showed that SVD is often less accurate than CA-ML and CB-SM (Chou et al., 2016; Molloy and Warnow, 2018). Still, the SVD inferences illustrated potentially conflicting topological alternatives.

In summary, phylogenetic inference of the three datasets (“raw”, “int_251-500”, and “int_301-450”) showed positive trends in terms of the resulting BS support values and concordance factor values with increasing degree of dataset reduction for CA-ML and CB-SM. The resulting SVD reconstructions, however, appeared to be impeded by information limitation and data bias.

4.3.3 Phylogenetic inference of the truncated locus datasets

In general, increasing locus length is associated with increasing phylogenetic information, lower GTEE and thus an increased accuracy of species tree estimation (e.g. Mirarab et al., 2014, 2016; Xi et al., 2015; Chou et al., 2016; Hosner et al., 2016; Xu and Yang, 2016; Blom et al., 2017; Molloy and Warnow, 2018). We expected a decrease in locus length to decrease the total and average phylogenetic information per locus, and consequently to

negatively affect performance. To test this, the "raw" assembly loci were truncated and used as input for CA-ML (Supplementary Figure S7 A and B) and CB-SM inference (Supplementary Figure S7 C and D).

The truncated datasets showed a 2/3 reduction in phylogenetic information (Table 1, "int_251-500_short" and "int_301-450_short"), resulted incongruently resolved tree topologies (Fig. S7), and yielded decreased estimated BS support and concordance factor values, while the factor value differences of the clade and backbone branches increased strongly compared to the original datasets (Table S10). Therefore, we conclude that the locus length reduction had a substantially negative impact on the phylogenetic inference. This is in line with findings by studies comparing the inference performance over varying locus lengths and information contents (e.g. Mirarab et al., 2014, 2016; Xi et al., 2015; Chou et al., 2016; Xu and Yang, 2016; Molloy and Warnow, 2018).

However, we performed a drastic locus length reduction by 2/3, which resulted in an average locus length of 120/123nt (Table 1). As we found during locus filtering (see 2.5) and phylogenetic inference of the resulting datasets, an average locus length of 373nt (±43nt) in an assembly range of 300-450nt yielded sufficient phylogenetic information per locus and in total for successful CB-SM inference. Other empirical studies using similar or even shorter length ranges also achieved a successful CB-SM inference of the assembled data (e.g. Curto et al., 2018; Rancilhac et al., 2019). Based on our results, and as found by numerous studies (e.g., Gatesy and Springer, 2014; Lanier et al., 2014; Liu et al., 2015; Xi et al., 2015; Hosner et al., 2016; Huang and Knowles, 2016; Blom et al., 2017; Sayyari et al., 2017; Xu and Yang, 2016; Lee et al., 2018), we suggest that locus quality in terms of the information content and its distribution across the assembly and taxa is of greater importance than mere locus length. Yet, this also strongly depends on the taxonomic level, i.e. sequence divergence, of the study group.

4.3.4 On the accuracy of the Aichryson phylogeny

The accuracy of the phylogenetic outcome is the suggested by the emerging congruence of the CA-ML and CB-SM reconstructions with increasing data quality. Inference of the "int_301-450" dataset yielded overall congruent, similarly well-supported topologies as well as similar concordance factor values and differences. In addition, the phylogenetic pattern matches the species distributions. For instance, the species occurring on Madeira (*A*. *divaricatum*, *A*. *dumosum*, *A*. *villosum*) and the two *A*. *tortuosum* subspecies occurring on the eastern Canary Islands, Lanzarote (subsp. *tortuosum*) and Fuerteventura (subsp. *bethencourtianum*), each form a monophyletic group. The polyphyletic status of the *A*. *pachycaulon* subspecies is also consistent with previous studies (Mort et al., 2002; Fairfield et al., 2004).

However, as Goethe put it: „We know accurately only when we know little; with knowledge, doubt increases" (von Goethe, 2012, published postum). 1) *Aichryson* is not a model group and lacks comparable studies in terms of data properties (locus length, sequence variation, missingness), data analysis (data assembly, locus filtering) and phylogenetic inference. 2) We did not statistically assess potential variation in phylogenetic inference of the filtered datasets using multiple replicates. 3) The extent to which phylogenetic inference may be impacted by terraces due to artificial conflicts among clades arising from the data structure herein is unclear (Sanderson et al., 2010, 2011, 2015; Simmons, 2012; Dobrin et al., 2018). 4) Although locus properties gained quality and sample coverage became more even, the low concordance factor values of some backbone branches representing the relationships of clades 2+3+4 to clade 5 and high concordance factor value differences of the within clade branches of clade 5 suggest a strong conflict among clades and taxa, respectively (Minh et al., 2020a, b). However, we cannot assess whether this incongruence of information among locus trees is a true biological signal due to reticulate evolution or an artifact of the data structure. 5) In addition, the ongoing, sometimes heated debate over the most accurate application, analysis, and inference of a variety of RRL/SRS-based approaches, along with a series of comparisons

of divergent concepts and opinions, further complicate the interpretation of the results (e.g. de Queiroz and Gatesy 2007; Edwards et al., 2007, 2016; Kubatko and Degnan 2007; Degnan and Rosenberg, 2009; Knowles, 2009; Leaché and Rannala, 2011; Song et al., 2012; Gatesy and Springer, 2013, 2014; Springer and Gatesy 2014, 2016, 2018; Mirarab et al., 2014b, 2015, 2016; Chou et al., 2015; Roch and Steel 2015; Mirarab and Warnow 2015; Solís-Lemus et al., 2016; Mendes and Hahn, 2018; Molloy and Warnow, 2018; Bryant and Hahn, 2020; Rannala et al., 2020). In particular, the inference accuracy of CA-ML in the presence of gene tree-species tree discordance (Degnan and Rosenberg, 2006, 2009; Kubatko and Degnan, 2007; Knowles, 2009; Roch and Steel, 2015; Solís-Lemus et al., 2016; Mendes and Hahn, 2018; Bryant and Hahn, 2020) and the performance of CB-SM under conditions of GTEE (Springer and Gatesy, 2014, 2016; Roch and Warnow, 2015; Xi et al., 2015, 2016; Solís-Lemus et al., 2016; Xu and Yang, 2016; Sayyari et al., 2017; Molloy and Warnow, 2018) raise concerns.

In general, CA-ML and CB-SM are expected to yield congruent results under less challenging conditions of gene tree-species tree discordance (Edwards et al., 2007; Kubatko and Degnan, 2007; Leaché and Rannala, 2011). Comparative studies showed that CA-ML and CB-SM performed equally under various levels of ILS, with CA-ML performing more accurate under challenging GTEE conditions (Chou et al., 2015; Xi et al., 2015, 2016; Mirarab et al., 2016; Sayyari et al., 2017; Molloy and Warnow, 2018). Moreover, inference of empirical data using both approaches generally yielded congruent results (e.g. Chiari et al., 2012; Hosner et al., 2016; Blom et al., 2017; Sayyari et al., 2017; Curto et al., 2018; Rancilhac et al., 2019). The bottom line is that we cannot ultimately assess the accuracy of the species tree for *Aichryson*, still, we construe the overall congruence as supporting the accuracy of the phylogenetic outcome.

4.4 Conclusion

The methodology presented in this study successfully led to a coalescent-based inference of our focal group *Aichryson*. For some, however, the series of approaches tested by us may be equivalent to a butcher making "phylogenetic sausage" (for the definition of a "phylogenetic sausage" see: Gatesy and Springer, 2014; see further: Springer and Gatesy, 2016, 2018; Bryant and Hahn, 2020; Fernández et al., 2020; Rannala et al., 2020). Admittedly, all methodological components could be modified and improved in many ways. The resulting data were also quite demanding to analyze. Still, particularly the challenging data structure provided the opportunity to gain further valuable insights to drive the development of fast and reliable RRL-SRS approaches. 1) Minor modifications of the RADseq toolbox regarding fragment size selection and sequencing range yielded a strongly reduced locus set of extended length. 2) Evaluation of a few metrics enabled an informed selection of clustering thresholds for data assembly within and across samples. 3) Simple descriptive statistics of the resulting assembly were useful for an initial assessment of the data structure. 4) Locus filtering greatly assisted to identify assembly areas of presumably biased locus and taxon coverage. 5) Comparative evaluation of phylogenetic patterns, such as terrace-like branches, BS support values and concordance factor values highlighted the importance of data quality over mere quantity, in particular for the coalescent-based summary method.

We are convinced that the combination of highly flexible RRL-SRS laboratory, data analysis, and inference approaches is crucial for a fast and reliable biodiversity exploration. Hence, we highly encourage the community to: 1) modify the extensive RADseq toolbox regarding an extended fragment length and sequencing range, 2) reduce the data quantity in favor of data quality, 3) utilize approaches guiding an informed threshold selection for accurate clustering, 4) thoroughly analyze and test the resulting assembly and locus properties for potential biases,

5) and to compare and evaluate the resulting phylogenetic trends using multiple inference approaches.

FUNDING

This work benefitted from the sharing of expertise on RADseq data in various groups of organisms at various taxonomic levels within the Deutsche Forschungsgemeinschaft DFG priority program SPP 1991 TaxonOMICS and from financial support from DFG KA 1816/11–1.

ACKNOWLEDGEMENTS

We thank the following people and institutions for providing materials for this study: Ángel Bañares Baudet (Tenerife), Stephan Scholz (Lanzarote), Stefan Abrahamczyk (Bonn) and Nadine Bobon (Mainz). We thank Hans Zischler (Mainz) and Dirk Albach (Oldenburg) for providing access to their lab facilities. We thank Oliver Hawlitschek and three further reviewers for helpful comments on the manuscript. We are grateful to Doris Franke and Maria Geyer for their assistance with the figure design, and to Christopher Wild for taking care of the living collection of Crassulaceae at the Botanical Garden Mainz.

This work used computing infrastructure of: -the Scientific Compute Cluster at the Göttingen Society for Scientific Data Processing (GWDG), as part of the joint data center of Max Planck Society for the Advancement of Science (MPG) and University of Göttingen, -the supercomputer Mogon at Johannes Gutenberg University Mainz, which is a member of the Alliance for High Performance Computing in Rhineland Palatinate (AHRP) and the Gauss Alliance e.V., and -the Center for Genome Research and Biocomputing at the Oregon State University. We gratefully acknowledge the computing time granted.

SEQUENCE DATA

Demultiplexed raw data is available at the NCBI Sequence Read Archive (www.ncbi.nlm.nih.gov/sra/PRJNA642981), BioProject PRJNA642981 (www.ncbi.nlm.nih.gov/bioproject/PRJNA642981).

APPENDIX AND SUPPLEMENT

Supplementary material available from Mendeley Data, doi: 10.17632/yb6fd93dbw.1.

Appendix 1: RADseq lab workflow.

Figure S1: ISC/BSC threshold selection, box- and scatter plots.

Figure S2: Phylogenetic inference of the unfiltered "raw" assembly.

Figure S3: Locus filtering by minimum number of samples, minimum variability and locus length intervals.

Figure S4: Locus filtering by increasing maximum locus length and locus length intervals.

Figure S5: Phylogenetic inference of the "int_251-500" dataset.

Figure S6: Phylogenetic inference of the "int_301-450" dataset.

Figure S7: Phylogenetic inference of the truncated datasets.

Table S1: Sampling and flow cytometry.

Table S2: Excerpt of the *in silico* digest for REase selection, adapter and primer sequences.

Table S3: Pipetting scheme for digest and ligation.

Table S4: Sequencing output, FastQC and MultiQC reports.

Table S5: *ipyrad* parameter settings.

1334 Table S6: Locus filtering by minimum number of samples, minimum variability and locus
1335 length intervals.

1336 Table S7: Locus filtering by increasing maximum locus length and locus length intervals.

1337 Table S8: ISC threshold selection and calculation of NPL.

1338 Table S9: Descriptive statistics of the "raw" assembly and subsequently selected datasets.

1339 Table S10: BS support and concordance factor values of the comparative phylogenetic
1340 inference.

1341 Supplementary data 1: ipyrad output files (loci and PHYLIP) of the unfiltered "raw"
1342 assembly.

1343 Supplementary data 2: NEXUS tree files of the locus filtering approach using CA-ML and
1344 CB-SM, of the comparative phylogenetic inference using CA-ML, CB-SM and SVD, and of
1345 the phylogenetic inference of the truncated locus datasets using CA-ML and CB-SM.

1346 REFERENCES

1347 Abeysinghe, P.D., Wijesinghe, K.G.G., Tachida, H., Yoshda, T., 2009. Molecular
1348 characterization of Cinnamon (*Cinnamomum verum* Presl) accessions and evaluation of
1349 genetic relatedness of Cinnamon species in Sri Lanka based on *trn*L intron region,
1350 intergenic spacers between *trn*T-*trn*L, *trn*L-*trn*F, *trn*H-*psb*A and nuclear ITS. Res. J. Agric.
1351 Biol. Sci. 5(6):1079–1088.

1352 Andrews, S., 2010. FastQC: a quality control tool for high throughput sequence data. Available
1353 from: http://www.bioinformatics.babraham.ac.uk/projects/fastqc/.

1354 Andrews, K.R., Good, J.M., Miller, M.R., Luikart, G., Hohenlohe, P.A., 2016. Harnessing the
1355 power of RADseq for ecological and evolutionary genomics. Nat. Rev. Genet. 17:81–92.
1356 doi: https://doi.org/10.1038/nrg.2015.28.

1357 Baird, N.A., Etter, P.D., Atwood, T.S., Currey, M.C., Shiver, A.L., Lewis, Z.A., Selker, E.U.,
1358 Cresko, W.A., Johnson, E.A., 2008. Rapid SNP discovery and genetic mapping using
1359 sequenced RAD markers. PloS one. 3(10): e3376. doi:
1360 https://doi.org/10.1371/journal.pone.0003376.

1361 Bañares Baudet, Á., 2002. On some poorly known taxa of *Aichryson* sect. *Aichryson* and *A.*
1362 *bituminosum* sp. nova (Crassulaceae). Willdenowia 32(2):221–230. doi:
1363 https://doi.org/10.3372/wi.32.32204.

1364 Bañares Baudet, Á., 2015a. Las plantas suculentas (Crassulaceae) endémicas de las Islas
1365 Canarias. Santa Cruz de Tenerife: Publicaciones Turquesa.

1366 Bañares Baudet, Á., 2015b. Híbridos de la familia Crassulaceae en las islas Canarias. V. Vieraea
1367 43:189–206.

1368 Bañares Baudet, Á., 2017. Typification of *Aichryson pachycaulon* subsp. *praetermissum* and
1369 description of *A. roseum* sp. nov. (Crassulaceae) from Gran Canaria, Canary Islands, Spain.
1370 Willdenowia 47(2):127–134. doi: https://doi.org/10.3372/wi.47.47204.

1371 Bayona-Vásquez, N.J., Glenn, T.C., Kieran, T.J., Pierson, T.W., Hoffberg, S.L., Scott, P.A.,
1372 Bentley, K.E., Finger, J.W., Louha, S., Troendle, N. and Díaz-Jaimes, P., Mauricio, R.,
1373 Faircloth, B.C., 2019. Adapterama III: Quadruple-indexed, double/triple-enzyme RADseq
1374 libraries (2RAD/3RAD). PeerJ 7:e7724. doi: https://doi.org/10.7717/peerj.7724.

1375 Bayzid, M. S., Warnow, T., 2013. Naive binning improves phylogenomic analyses.
1376 Bioinformatics 29: 2277–2284. doi: https://doi.org/10.1093/bioinformatics/btt394.

1377 Blom, M.P.K., Bragg, J.G., Potter, S., Moritz, C., 2017. Accounting for uncertainty in gene tree
1378 estimation: summary-coalescent species tree inference in a challenging radiation of
1379 Australian lizards. Syst. Biol. 66:352–366. doi: https://doi.org/10.1093/sysbio/syw089.

1380 Bouckaert, R., Heled, J., Kühnert, D., Vaughan, T., Wu, C.-H., Xie, D., Suchard, M.A.,
1381 Rambaut, A, Drummond, A.J., 2014. BEAST 2: a software platform for Bayesian
1382 evolutionary analysis. PLoS Comp. Biol. 10(4):e1003537. doi:
1383 https://doi.org/10.1371/journal.pcbi.1003537.

1384 Bryant, D., Hahn, M.W., 2020. The Concatenation Question. In: Scornavacca, C., Delsuc, F.,
1385 Galtier, N., editors, Phylogenetics in the Genomic Era, chapter No. 3.4, pp. 3.4:1–3.4:23.
1386 No commercial publisher | Authors open access book. The book is freely available at
1387 https://hal.inria.fr/PGE. HAL Id: hal-02535651.

1388 Bryant, D., Bouckaert, R., Felsenstein, J., Rosenberg, N.A., RoyChoudhury, A., 2012. Inferring
1389 species trees directly from biallelic genetic markers: bypassing gene trees in a full
1390 coalescent analysis. Molec. Biol. Evol. 29(8):1917–1932. doi:
1391 https://doi.org/10.1093/molbev/mss086.

1392 Buono, D., Khan, G., von Hagen, K.B., Kosachev, P.A., Mayland-Quellhorst, E., Mosyakin, S.
1393 L., Albach, D.C., 2021. Comparative Phylogeography of Veronica spicata and V. longifolia
1394 (Plantaginaceae) Across Europe: Integrating Hybridization and Polyploidy in
1395 Phylogeography. Front. Plant. Sci. 11, 588354. doi:
1396 https://doi.org/10.3389/fpls.2020.588354.

1397 Burleigh, J.G., Kimball, R.T., Braun, E.L., 2015. Building the avian tree of life using a large-
1398 scale, sparse supermatrix. Mol. Phylogenet. Evol. 84: 53-63. doi:
1399 https://doi.org/10.1016/j.ympev.2014.12.003.

1400 Camacho, C., Coulouris, G., Avagyan, V., Ma, N., Papadopoulos, J., Bealer, K., Madden, T.L.,
1401 2009. BLAST+: architecture and applications. BMC Bioinf. 10:421. doi:
1402 http://dx.doi.org/10.1186/1471-2105-10-421.

1403 Catchen, J., Hohenlohe, P.A., Bassham, S., Amores, A., Cresko, W.A., 2013. Stacks: an
1404 analysis tool set for population genomics. Molec. Ecol. 22(11):3124–3140. doi:
1405 https://doi.org/10.1111/mec.12354.

1406 Chen, M.Y., Liang, D., Zhang, P., 2015. Selecting question-specific genes to reduce
1407 incongruence in phylogenomics: a case study of jawed vertebrate backbone phylogeny.
1408 Syst. Biol. 64(6): 1104-1120. doi: https://doi.org/10.1093/sysbio/syv059.

1409 Chernomor, O., Von Haeseler, A., Minh, B.Q., 2016. Terrace aware data structure for
1410 phylogenomic inference from supermatrices. Syst. Biol. 65(6): pp.997-1008. doi:
1411 https://doi.org/10.1093/sysbio/syw037.

1412 Chiari, Y., Cahais, V., Galtier, N., Delsuc, F., 2012. Phylogenomic analyses support the
1413 position of turtles as the sister group of birds and crocodiles (Archosauria). Bmc Biology.
1414 10(1): 1-15. doi: https://doi.org/10.1186/1741-7007-10-65.

1415 Chifman, J., Kubatko, L., 2014. Quartet inference from SNP data under the coalescent model.
1416 Bioinformatics 30(23):3317–3324. doi: https://doi.org/10.1093/bioinformatics/btu530.

1417 Chou, J., Gupta, A., Yaduvanshi, S., Davidson, R., Nute, M., Mirarab, S., Warnow, T., 2015.
1418 A comparative study of SVDquartets and other coalescent-based species tree estimation
1419 methods. BMC Genomics 16:S2. doi: https://doi.org/10.1186/1471-2164-16-S10-S2.

1420 Crotti, M., Barratt, C.D., Loader, S.P., Gower, D.J., Streicher, J.W., 2019. Causes and analytical
1421 impacts of missing data in RADseq phylogenetics: insights from an African frog
1422 (*Afrixalus*). Zool. Scripta 48(2):157–167. doi: https://doi.org/10.1111/zsc.12335.

1423 Curto, M., Schachtler, C., Puppo, P., Meimberg, H., 2018. Using a new RAD-sequencing
1424 approach to study the evolution of *Micromeria* in the Canary islands. Molec. Phylogen.
1425 Evol. 119:160–169. doi: https://doi.org/10.1016/j.ympev.2017.11.005.

1426 de Oca, A.N.M., Barley, A.J., Meza-Lázaro, R.N., García-Vázquez, U.O., Zamora-Abrego,
1427 J.G., Thomson, R.C., Leaché, A.D., 2017. Phylogenomics and species delimitation in the
1428 knob-scaled lizards of the genus Xenosaurus (Squamata: Xenosauridae) using ddRADseq
1429 data reveal a substantial underestimation of diversity. Molec. Phylogen. Evol. 106:241-253.
1430 doi: https://doi.org/10.1016/j.ympev.2016.09.001.

1431 de Queiroz, A., Donoghue, M.J., Kim, J., 1995. Separate versus combined analysis of
1432 phylogenetic evidence. Annu. Rev. Ecol. Syst.. 26(1): 657-681. Stable URL:
1433 https://www.jstor.org/stable/2097223

1434 de Queiroz, A., Gatesy, J., 2007. The supermatrix approach to systematics. Trends Ecol. Evol,
1435 22(1): 34-41. doi: https://doi.org/10.1016/j.tree.2006.10.002

1436 Degnan, J.H., Rosenberg, N.A., 2006. Discordance of species trees with their most likely gene
1437 trees. PLoS Genet. 2(5):e68. doi: https://doi.org/10.1371/journal.pgen.0020068.

1438 Degnan J.H., Rosenberg N.A., 2009. Gene tree discordance, phylogenetic inference and the
1439 multispecies coalescent. Trends Ecol. Evol. 24(6):332–340. doi:
1440 https://doi.org/10.1016/j.tree.2009.01.009.

1441 Dillenberger, M.S., Kadereit, J.W., 2017. Simultaneous speciation in the European high
1442 mountain flowering plant genus *Facchinia* (*Minuartia* s.l., Caryophyllaceae) revealed by
1443 genotyping-by-sequencing. Molec. Phylogen. Evol. 112:23–35. doi:
1444 https://doi.org/10.1016/j.ympev.2017.04.016.

1445 Dobrin, B.H., Zwickl, D.J., Sanderson, M.J., 2018. The prevalence of terraced treescapes in
1446 analyses of phylogenetic data sets. BMC Evol. Biol. 18(1): 1-16. doi:
1447 https://doi.org/10.1186/s12862-018-1162-9.

1448 Duan, L., Wen, J., Yang, X., Liu, P.L., Arslan, E., Ertuğrul, K., Chang, Z.Y., 2015. Phylogeny
1449 of *Hedysarum* and tribe Hedysareae (Leguminosae: Papilionoideae) inferred from sequence
1450 data of ITS, *matK*, *trnL-F* and *psbA-trnH*. Taxon 64(1):49–64. doi:
1451 https://doi.org/10.12705/641.26.

1452 Eaton, D.A., Overcast, I., 2020. ipyrad: Interactive assembly and analysis of RADseq
1453 datasets. Bioinformatics, 36(8): 2592-2594. doi:
1454 https://doi.org/10.1093/bioinformatics/btz966

1455 Eaton, D.A.R., Ree, R.H., 2013. Inferring phylogeny and introgression using RADseq data: an
1456 example from flowering plants (*Pedicularis*: Orobanchaceae). Syst. Biol. 62(5):689–706.
1457 doi: https://doi.org/10.1093/sysbio/syt032.

1458 Eaton, D.A.R., Spriggs, E.L., Park, B., Donoghue, M.J., 2017. Misconceptions on missing data
1459 in RAD-seq phylogenetics with a deep-scale example from flowering plants. Syst. Biol.
1460 66(3):399–412. doi: https://doi.org/10.1093/sysbio/syw092.

1461 Edwards, S.V., Liu, L., Pearl, D.K., 2007. High-resolution species trees without concatenation.
1462 P. Nati. A. Sci. USA. 104(14): pp.5936-5941. doi:
1463 https://doi.org/10.1073/pnas.0607004104.

1464 Edwards, S.V., Xi, Z., Janke, A., Faircloth, B.C., McCormack, J.E., Glenn, T.C., Zhong, B.,
1465 Wu, S., Lemmon, E.M., Lemmon, A.R. and Leaché, A.D., 2016. Implementing and testing
1466 the multispecies coalescent model: a valuable paradigm for phylogenomics. Mol.
1467 Phylogenet. Evol. 94: 447-462. doi: https://doi.org/10.1016/j.ympev.2015.10.027.

1468 Eggli, U., 2008. Sukkulenten. 2nd Edition. Stuttgart: Eugen Ulmer KG.

1469 Elshire, R.J., Glaubitz, J.C., Sun, Q., Poland, J.A., Kawamoto, K., Buckler, E.S., Mitchell, S.E.,
1470 2011. A robust, simple genotyping-by-sequencing (GBS) approach for high diversity
1471 species. PLoS One 6(5):e19379. doi: https://doi.org/10.1371/journal.pone.0019379.

1472 Escudero, M., Eaton, D.A.R., Hahn, M., Hipp, A.L., 2014. Genotyping-by-sequencing as a tool
1473 to infer phylogeny and ancestral hybridization: a case study in *Carex* (Cyperaceae). Molec.
1474 Phylogen. Evol. 79:359–367. doi: https://doi.org/10.1016/j.ympev.2014.06.026.

1475 Ewels, P., Magnusson, M., Lundin, S., Käller, M., 2016. MultiQC: summarize analysis results
1476 for multiple tools and samples in a single report. Bioinformatics 32(19): 3047-3048. doi:
1477 https://doi.org/10.1093/bioinformatics/btw354.

1478 Fairfield, K.N., Mort, M.E., Santos-Guerra, A., 2004. Phylogenetics and evolution of the
1479 Macaronesian members of the genus *Aichryson* (Crassulaceae) inferred from nuclear and
1480 chloroplast sequence data. Pl. Syst. Evol. 248:71–83. doi: https://doi.org/10.1007/s00606-
1481 004-0190-7.

1482 Fernández, R., Gabaldón, T., Dessimoz, C., 2020. Orthology: definitions, inference, and
1483 impact on species phylogeny inference. In Scornavacca, C., Delsuc, F., and Galtier, N.,
1484 editors, Phylogenetics in the Genomic Era, chapter No. 2.4, pp. 2.4:1–2.4:14. No

commercial publisher | Authors open access book. The book is freely available at https://hal.inria.fr/PGE. HAL Id: hal-02535414

Gatesy, J., Springer, M.S., 2013. Concatenation versus coalescence versus "concatalescence". P. Natl. Acad. Sci. USA, 110(13): E1179-E1179. doi: https://doi.org/10.1073/pnas.1221121110.

Gatesy, J., Springer, M.S., 2014. Phylogenetic analysis at deep timescales: unreliable gene trees, bypassed hidden support, and the coalescence/concatalescence conundrum. Mol. Phylogenet. Evol.. 80: 231-266. doi: https://doi.org/10.1016/j.ympev.2014.08.013

Gerschwitz-Eidt, M.A., Kadereit, J.W., 2019. Genotyping-by-sequencing (GBS), ITS and cpDNA phylogenies reveal the existence of a distinct Pyrenean/Cantabrian lineage in the European high mountain genus *Homogyne* (Asteraceae) and imply dual westward migration of the genus. Alp. Botany 129(1):21–31. doi: https://doi.org/10.1007/s00035-018-0212-7.

Good, J.M., 2012. Reduced representation methods for subgenomic enrichment and next-generation sequencing. In: Orgogozo V., Rockman M.V., editors. Methods in Molecular Biology Vol. 772: Molecular Methods for Evolutionary Genetics. New York: Humana Press. p. 85–103. doi: https://doi.org/10.1007/978-1-61779-228-1_5.

Grover, C. E., Salmon, A., Wendel, J. F., 2012. Targeted sequence capture as a powerful tool for evolutionary analysis1. Am. J. Botany. 99(2). 312-319. doi: https://doi.org/10.3732/ajb.1100323.

Hamon, P., Grover, C.E., Davis, A.P., Rakotomalala, J.J., Raharimalala, N.E., Albert, V.A., Sreenath, H.L., Stoffelen, P., Mitchell, S.E., Couturon, E., Hamon, S., 2017. Genotyping-by-sequencing provides the first well-resolved phylogeny for coffee (Coffea) and insights into the evolution of caffeine content in its species: GBS coffee phylogeny and the

1509 evolution of caffeine content. Molec. Phylogen. Evol. 109. pp.351-361. doi:
1510 https://doi.org/10.1016/j.ympev.2017.02.009.

1511 Harvey, M.G., Judy, C.D., Seeholzer, G.F., Maley, J.M., Graves, G.R., Brumfield, R.T., 2015.
1512 Similarity thresholds used in DNA sequence assembly from short reads can reduce the
1513 comparability of population histories across species. PeerJ 3:e895. doi:
1514 https://doi.org/10.7717/peerj.895.

1515 Harvey, M.G., Smith, B.T., Glenn, T.C., Faircloth, B.C., Brumfield, R.T., 2016. Sequence
1516 capture versus restriction site associated DNA sequencing for shallow systematics. Syst.
1517 Biol. 65(5):910–924. doi: https://doi.org/10.1093/sysbio/syw036.

1518 Heled, J., Drummond, A.J., 2009. Bayesian inference of species trees from multilocus data.
1519 Molec. Bio. Evol. 27(3):570–580. doi: https://doi.org/10.1093/molbev/msp274.

1520 Herrera, S., Shank, T.M., 2016. RAD sequencing enables unprecedented phylogenetic
1521 resolution and objective species delimitation in recalcitrant divergent taxa. Molec.
1522 Phylogen. Evol. 100:70–79. doi: https://doi.org/10.1016/j.ympev.2016.03.010.

1523 Hipp, A.L., Manos, P.S., Hahn, M., Avishai, M., Bodénès, C., Cavender-Bares, J., Crowl, A.A.,
1524 Deng, M., Denk, T., Fitz-Gibbon, S., Gailing, O., 2020. Genomic landscape of the global
1525 oak phylogeny. New Phytol. 226(4). pp.1198-1212. doi:
1526 https://doi.org/10.1111/nph.16162.

1527 Hirsch, C.N., Buell, C.R., 2013. Tapping the promise of genomics in species with complex,
1528 nonmodel genomes. Annual Rev. Pl. Biol. 64:89–110. doi:
1529 https://doi.org/10.1146/annurev-arplant-050312-120237.

1530 Hosner, P.A., Faircloth, B.C., Glenn, T.C., Braun, E.L. and Kimball, R.T., 2016. Avoiding
1531 missing data biases in phylogenomic inference: an empirical study in the landfowl (Aves:

1532 Galliformes). Mol. Biol. Evol. 33(4): 1110-1125. doi:
1533 https://doi.org/10.1093/molbev/msv347.

1534 Huang H., Knowles, L.L., 2016. Unforeseen consequences of excluding missing data from
1535 next-generation sequences: simulation study of RAD sequences. Syst. Biol. 65(3):357–365.
1536 doi: https://doi.org/10.1093/sysbio/syu046.

1537 Ilut, D.C., Nydam, M.L., Hare, M.P., 2014. Defining loci in restriction-based reduced
1538 representation genomic data from nonmodel species: sources of bias and diagnostics for
1539 optimal clustering. BioMed Res. Int. 2014:675158. doi:
1540 http://dx.doi.org/10.1155/2014/675158.

1541 Karbstein, K., Tomasello, S., Hodač, L., Dunkel, F. G., Daubert, M., & Hörandl, E., 2020.
1542 Phylogenomics supported by geometric morphometrics reveals delimitation of sexual
1543 species within the polyploid apomictic Ranunculus auricomus complex (Ranunculaceae).
1544 Taxon. 69(6): 1191-1220. doi: https://doi.org/10.1002/tax.12365.

1545 Karbstein, K., Tomasello, S., Hodač, L., Lorberg, E., Daubert, M., Hörandl, E., 2021. Moving
1546 beyond assumptions: Polyploidy and environmental effects explain a geographical
1547 parthenogenesis scenario in European plants. Mol. Ecol. doi:
1548 https://doi.org/10.1111/mec.15919.

1549 Knowles, L.L., 2009. Estimating species trees: methods of phylogenetic analysis when there is
1550 incongruence across genes. Syst. Biol. 58(5):463–467. doi:
1551 https://doi.org/10.1093/sysbio/syp061.

1552 Kubatko, L.S., Degnan J.H., 2007. Inconsistency of phylogenetic estimates from concatenated
1553 data under coalescence. Syst. Biol. 56(1):17–24. doi:
1554 https://doi.org/10.1080/10635150601146041.

1555 Kumar, S., Filipski, A.J., Battistuzzi, F.U., Kosakovsky Pond, S.L., Tamura, K., 2012. Statistics
1556 and truth in phylogenomics. Molec. Biol. Evol. 29(2): pp.457-472. doi:
1557 https://doi.org/10.1093/molbev/msr202.

1558 Kück, P., Meusemann, K., 2010. FASconCAT: convenient handling of data matrices. Molec.
1559 Phylogenet. Evol. 56(3): 1115-1118. doi: https://doi.org/10.1016/j.ympev.2010.04.024.

1560 Kück, P., Longo, G.C., 2014. FASconCAT-G: extensive functions for multiple sequence
1561 alignment preparations concerning phylogenetic studies. Front. Zool. 11:81. doi:
1562 https://doi.org/10.1186/s12983-014-0081-x.

1563 Lanier, H.C., Huang, H., Knowles, L.L., 2014. How low can you go? The effects of mutation
1564 rate on the accuracy of species-tree estimation. Mol. Phylogenet. Evol. 70: 112-119. doi:
1565 https://doi.org/10.1016/j.ympev.2013.09.006.

1566 Leaché, A.D., Rannala, B., 2011. The accuracy of species tree estimation under simulation: a
1567 comparison of methods. Syst. Biol. 60(2): 126-137. doi:
1568 https://doi.org/10.1093/sysbio/syq073.

1569 Lee, K.M., Kivelä, S.M., Ivanov, V., Hausmann, A., Kaila, L., Wahlberg, N., Mutanen, M.,
1570 2018. Information dropout patterns in restriction site associated DNA phylogenomics and
1571 a comparison with multilocus Sanger data in a species-rich moth genus. Syst. Biol.
1572 67(6):925–939. doi: https://doi.org/10.1093/sysbio/syy029.

1573 Lepais, O., Weir, J.T., 2014. Sim RAD: an R package for simulation-based prediction of the
1574 number of loci expected in RAD seq and similar genotyping by sequencing approaches.
1575 Mol. Ecol. Resour. 14(6): 1314-1321. doi: https://doi.org/10.1111/1755-0998.12273.

1576 Liu, L., 2008. BEST: Bayesian estimation of species trees under the coalescent model.
1577 Bioinformatics. 24(21): 2542-2543. doi: https://doi.org/10.1093/bioinformatics/btn484.

1578 Liu, L., Xi, Z., Wu, S., Davis, C., Edwards, S.V., 2015. Estimating phylogenetic trees from
1579 genome-scale data. Ann. N. Y. Acad. Sci. 1360: 36–53. doi: 10.1111/nyas.12747.

1580 Long, C., Kubatko, L., 2018. The effect of gene flow on coalescent-based species-tree
1581 inference. Syst. Biol. 67(5):770–785. doi: https://doi.org/10.1093/sysbio/syy020.

1582 MacConaill, L.E., Burns, R.T., Nag, A., Coleman, H.A., Slevin, M.K., Giorda, K., Light, M.,
1583 Lai, K., Jarosz, M., McNeill, M.S., Ducar, M.D., 2018. Unique, dual-indexed sequencing
1584 adapters with UMIs effectively eliminate index cross-talk and significantly improve
1585 sensitivity of massively parallel sequencing. BMC genomics, 19(1): 1-10. doi:
1586 https://doi.org/10.1186/s12864-017-4428-5.

1587 Maddison, W. P., 1997. Gene trees in species trees. Syst, Biol. 46(3): 523-536. doi:
1588 https://doi.org/10.1093/sysbio/46.3.523.

1589 Maddison, W.P., Knowles, L.L., 2006. Inferring phylogeny despite incomplete lineage
1590 sorting. Syst. Biol. 55(1):21-30. doi: https://doi.org/10.1080/10635150500354928.

1591 Mamanova, L., Coffey, A.J., Scott, C.E., Kozarewa, I., Turner, E.H., Kumar, A., Howard, E.,
1592 Shendure, J., Turner, D.J., 2010. Target-enrichment strategies for next-generation
1593 sequencing. Nat. Methods. 7(2). p.111. doi: https://doi.org/10.1038/nmeth.1419.

1594 Mardis, E., 2017. DNA sequencing technologies: 2006–2016. Nat. Protoc. 12:213–218. doi:
1595 https://doi.org/10.1038/nprot.2016.182.

1596 Martin, M., 2011. Cutadapt removes adapter sequences from high-throughput sequencing reads.
1597 EMBnet.journal 17(1):10–12. doi: https://doi.org/10.14806/ej.17.1.200.

1598 Mastretta-Yanes, A., Arrigo, N., Alvarez, N., Jorgensen, T.H., Piñero, D., Emerson, B.C., 2015.
1599 Restriction site-associated DNA sequencing, genotyping error estimation and de novo
1600 assembly optimization for population genetic inference. Mol. Ecol. Resour. 15(1): 28–41.
1601 doi: https ://doi.org/10.1111/1755-0998.12291

McCartney-Melstad, E., Gidiş, M., Shaffer, H. B., 2019. An empirical pipeline for choosing the optimal clustering threshold in RADseq studies. Molec. Ecol. Resour. 19(5). 1195-1204. doi: https://doi.org/10.5281/zenodo.2540263.

McCormack, J.E., Harvey, M.G., Faircloth, B.C., Crawford, N.G., Glenn, T.C., Brumfield, R.T., 2013a. A phylogeny of birds based on over 1,500 loci collected by target enrichment and high-throughput sequencing. PloS One 8(1):e54848. doi: https://doi.org/10.1371/journal.pone.0054848.

McCormack, J.E., Hird, S.M., Zellmer, A.J., Carstens, B.C., Brumfield, R.T., 2013b. Applications of next-generation sequencing to phylogeography and phylogenetics. Molec. Phylogen. Evol. 66(2):526–538. doi: https://doi.org/10.1016/j.ympev.2011.12.007.

McKain, M.R., Johnson, M.G., Uribe-Convers, S., Eaton, D., Yang, Y., 2018. Practical considerations for plant phylogenomics. Appl. Plant Sci. 6(3):e1038. doi: https://doi.org/10.1002/aps3.1038.

McKinney, G.J., Waples, R.K., Seeb, L.W., Seeb, J.E., 2017. Paralogs are revealed by proportion of heterozygotes and deviations in read ratios in genotyping-by-sequencing data from natural populations. Mol. Ecol. Resour. 17(4): 656–669. doi: https://doi.org/10.1111/1755-0998.12613

Mendes, F.K., Hahn, M.W., 2018. Why concatenation fails near the anomaly zone. Syst. Biol. 67(1): 158-169. doi: https://doi.org/10.1093/sysbio/syx063.

Messerschmid, T.F.E., Klein, J.T., Kadereit, G., Kadereit, J.W., 2020. Linnaeus' folly – phylogeny, evolution and classification of Sedum (Crassulaceae) and Crassulaceae subfamily Sempervivoideae. Taxon, 69(5), 892-926. doi: https://doi.org/10.1002/tax.12316.

1625 Miller, J.T., Grimes, J.W., Murphy, D.J., Bayer, R.J., Ladiges, P.Y., 2003. A phylogenetic
1626 analysis of the Acacieae and Ingeae (Mimosoideae: Fabaceae) based on *trnK*, *matK*, *psbA-*
1627 *trnH*, and *trnL/trnF* sequence data. Syst. Bot. 28(3):558–566. doi:
1628 https://doi.org/10.1043/02-48.1.

1629 Miller, M.R., Dunham, J.P., Amores, A., Cresko, W.A., Johnson, E.A., 2007. Rapid and cost-
1630 effective polymorphism identification and genotyping using restriction site associated
1631 DNA (RAD) markers. Genome Res. 17(2): 240-248. doi:
1632 http://www.genome.org/cgi/doi/10.1101/gr.5681207.

1633 Minh, B.Q., Hahn, M.W., Lanfear, R., 2020a. New methods to calculate concordance factors
1634 for phylogenomic datasets. Mol. Biol. Evol. 37(9): 2727-2733. doi:
1635 https://doi.org/10.1093/molbev/msaa106.

1636 Minh, B.Q., Schmidt, H.A., Chernomor, O., Schrempf, D., Woodhams, M.D., Von Haeseler,
1637 A., Lanfear, R., 2020b. IQ-TREE 2: New models and efficient methods for phylogenetic
1638 inference in the genomic era. Mol. Biol. Evol. 37(5): 1530-1534. doi:
1639 https://doi.org/10.1093/molbev/msaa015.

1640 Mirarab, S., Reaz, R., Bayzid, M.S., Zimmermann, T., Swenson, M.S., and Warnow, T., 2014a.
1641 ASTRAL: genome-scale coalescent-based species tree estimation. Bioinformatics,
1642 30(17):i541– i548. doi: https://doi.org/10.1093/bioinformatics/btu462.

1643 Mirarab, S., Bayzid, M.S., B. Boussau, B., Warnow, T., 2014b. Statistical binning enables an
1644 accurate coalescent-based estimation of the avian tree. Science 346: 1250463. doi:
1645 https://doi.org/10.1126/science.1250463.

1646 Mirarab S., Warnow T., 2015. ASTRAL-II: coalescent-based species tree estimation with many
1647 hundreds of taxa and thousands of genes. Bioinformatics 31(12):i44–i52. doi:
1648 https://doi.org/10.1093/bioinformatics/btv234.

1649 Mirarab, S., Bayzid, M.S., Warnow, T., 2016. Evaluating summary methods for multilocus
1650 species tree estimation in the presence of incomplete lineage sorting. Syst. Biol. 65(3):366–
1651 380. doi: https://doi.org/10.1093/sysbio/syu063.

1652 Molloy, E.K., Warnow, T., 2018. To include or not to include: the impact of gene filtering on
1653 species tree estimation methods. Syst. Biol. 67(2):285–303. doi:
1654 https://doi.org/10.1093/sysbio/syx077.

1655 Mora-Márquez, F., García-Olivares, V., Emerson, B.C., López de Heredia, U., 2017.
1656 ddradseqtools: a software package for in silico simulation and testing of double-digest RAD
1657 seq experiments. Mol. Ecol. Resour. 17(2): 230-246. doi : https://doi.org/10.1111/1755-
1658 0998.12550.

1659 Mort, M.E., Soltis, D.E., Soltis, P.S., Francisco-Ortega, J., Santos-Guerra, A., 2002.
1660 Phylogenetics and evolution of the Macaronesian clade of Crassulaceae inferred from
1661 nuclear and chloroplast sequence data. Syst. Bot. 27(2):271–288. doi:
1662 https://doi.org/10.1043/0363-6445-27.2.271.

1663 Moura, M., Carine, M., De Sequeira, M.M., 2015. *Aichryson santamariensis* (Crassulaceae): a
1664 new species endemic to Santa Maria in the Azores. Phytotaxa 234(1):37–50. doi:
1665 https://doi.org/10.11646/phytotaxa.234.1.2.

1666 Nicholls, J.A., Pennington, R.T., Koenen, E.J., Hughes, C.E., Hearn, J., Bunnefeld, L., Dexter,
1667 K.G., Stone, G.N., Kidner, C.A., 2015. Using targeted enrichment of nuclear genes to
1668 increase phylogenetic resolution in the neotropical rain forest genus Inga (Leguminosae:
1669 Mimosoideae). Front. Plant Sci. 6. p.710. doi : https://doi.org/10.3389/fpls.2015.00710.

1670 Nielsen, R., Paul, J.S., Albrechtsen, A., Song, Y.S., 2011. Genotype and SNP calling from next-
1671 generation sequencing data. Nat. Rev. Genet. 12(6):443–451. doi:
1672 https://doi.org/10.1038/nrg2986.

1673 Paetzold, C., Wood, K.R., Eaton, D.A., Wagner, W.L., Appelhans, M.S., 2019. Phylogeny of
1674 Hawaiian Melicope (Rutaceae): RAD-seq resolves species relationships and reveals ancient
1675 introgression. Front. Plant. Sci. 10, 1074. doi: https://doi.org/10.3389/fpls.2019.01074.

1676 Parchman, T.L., Jahner, J.P., Uckele, K.A., Galland, L.M., Eckert, A.J., 2018. RADseq
1677 approaches and applications for forest tree genetics. Tree Genet. Genomes. 14(3): 39. doi:
1678 https://doi.org/10.1007/s11295-018-1251-3.

1679 Pamilo, P., Nei, M., 1988. Relationships between gene trees and species trees. Mol. Biol. Evol.
1680 5(5): 568-583. doi: https://doi.org/10.1093/oxfordjournals.molbev.a040517.

1681 Paris, J.R., Stevens, J.R., Catchen, J.M., 2017. Lost in parameter space: a road map for stacks.
1682 Methods Ecol. Evol. 8(10):1360–1373. doi: https://doi.org/10.1111/2041-210X.12775.

1683 Pease, J.B., Brown, J.W., Walker, J.F., Hinchliff, C.E. and Smith, S.A., 2018. Quartet Sampling
1684 distinguishes lack of support from conflicting support in the green plant tree of life. Am. J.
1685 Bot. 105(3), pp.385-403. doi: https://doi.org/10.1002/ajb2.1016.

1686 Peterson, B.K., Weber, J.N., Kay, E.H., Fisher, H.S., Hoekstra, H.E., 2012. Double digest
1687 RADseq: an inexpensive method for de novo SNP discovery and genotyping in model and
1688 non-model species. PLoS One 7(5):e37135. doi:
1689 https://doi.org/10.1371/journal.pone.0037135.

1690 Puritz, J.B., Hollenbeck, C.M., Gold, J.R., 2014. dDocent: a RADseq, variant-calling pipeline
1691 designed for population genomics of non-model organisms. PeerJ 2:e431. doi:
1692 https://doi.org/10.7717/peerj.431.

1693 Rancilhac, L., Goudarzi, F., Gehara, M., Hemami, M. R., Elmer, K. R., Vences, M., Steinfarz,
1694 S., 2019. Phylogeny and species delimitation of near Eastern Neurergus newts
1695 (Salamandridae) based on genome-wide RADseq data analysis. Mol. Phylogenet. Evol.
1696 133, 189-197. doi: https://doi.org/10.1016/j.ympev.2019.01.003.

1697 Rannala, B., Edwards, S.V., Leaché, A., Yang, Z., 2020. The Multispecies Coalescent Model
1698 and Species Tree Inference. In Scornavacca, C., Delsuc, F., and Galtier, N., editors,
1699 Phylogenetics in the Genomic Era, chapter No. 3.3, pp. 3.3:1–3.3:21. No commercial
1700 publisher | Authors open access book. The book is freely available at
1701 https://hal.inria.fr/PGE. HAL Id: hal-02535622.

1702 Razkin, O., Sonet, G., Breugelmans, K., Madeira, M.J., Gómez-Moliner, B.J., Backeljau, T.,
1703 2016. Species limits, interspecific hybridization and phylogeny in the cryptic land snail
1704 complex Pyramidula: the power of RADseq data. Mol. Phylogenet. Evol. 101: 267-278.
1705 doi: https://doi.org/10.1016/j.ympev.2016.05.002.

1706 Ree, R.H., Hipp, A.L., 2015. Inferring phylogenetic history from restriction site associated
1707 DNA (RADseq). In: Hörandl E., Appelhans M.S., editors. Regnum Vegetabile Vol. 158:
1708 Next-Generation Sequencing in Plant Systematics. Oberreifenberg: Koeltz Scientific
1709 Books. p. 181–204.

1710 Reuter, J.A., Spacek, D.V., Snyder, M.P., 2015. High-throughput sequencing technologies.
1711 Molec. Cell. 58(4):586–597. doi: https://doi.org/10.1016/j.molcel.2015.05.004.

1712 Rivera-Colón, A.G., Rochette, N.C., Catchen, J.M., 2021. Simulation with RADinitio improves
1713 RADseq experimental design and sheds light on sources of missing data. Mol. Ecol.
1714 Resour. 21(2): 363-378. doi: https://doi.org/10.1111/1755-0998.13163.

1715 Roch, S., Steel, M., 2015. Likelihood-based tree reconstruction on a concatenation of aligned
1716 sequence data sets can be statistically inconsistent. Theor. Populat. Biol. 100:56–62. doi:
1717 https://doi.org/10.1016/j.tpb.2014.12.005.

1718 Roch, S., Warnow, T. 2015. On the robustness to gene tree estimation error (or lack thereof) of
1719 coalescent-based species tree methods. Syst. Biol. 64(4):663–676. doi:
1720 https://doi.org/10.1093/sysbio/syv016.

1721 Rubin, B.E., Ree, R.H., Moreau, C.S., 2012. Inferring phylogenies from RAD sequence data.
1722 PloS One 7(4):e33394. doi: https://doi.org/10.1371/journal.pone.0033394.

1723 Sanderson, M.J., McMahon, M.M., Steel, M., 2010. Phylogenomics with incomplete taxon
1724 coverage: the limits to inference. BMC Evol. Biol. 10(1): 1-13. doi:
1725 https://doi.org/10.1186/1471-2148-10-155.

1726 Sanderson, M.J., McMahon, M.M., Steel, M., 2011. Terraces in phylogenetic tree space.
1727 Science. 333(6041): 448-450. doi: 10.1126/science.1206357.

1728 Sanderson, M.J., McMahon, M.M., Stamatakis, A., Zwickl, D.J., Steel, M., 2015. Impacts of
1729 terraces on phylogenetic inference. Syst. Biol. 64(5): 709-726. doi:
1730 https://doi.org/10.1093/sysbio/syv024.

1731 Sayyari, E., and Mirarab, S., 2016. Fast coalescent-based computation of local branch support
1732 from quartet frequencies. Molec. Biol. Evol. 33(7): 1654-1668. doi:
1733 https://doi.org/10.1093/molbev/msw079.

1734 Sayyari, E., Whitfield, J. B., Mirarab, S., 2017. Fragmentary gene sequences negatively impact
1735 gene tree and species tree reconstruction. Molec. Biol. Evol. 34(12), 3279-3291. doi:
1736 https://doi.org/10.1093/molbev/msx261.

1737 Schmid, S., Genevest, R., Gobet, E., Suchan, T., Sperisen, C., Tinner, W., Alvarez, N., 2017.
1738 Hy RAD-X, a versatile method combining exome capture and RAD sequencing to extract
1739 genomic information from ancient DNA. Methods Ecol. Evol. 8(10): 1374-1388. doi:
1740 https://doi.org/10.1111/2041-210X.12785.

1741 Seo, T.K., 2008. Calculating bootstrap probabilities of phylogeny using multilocus sequence
1742 data. Molec. Biol. Evol. 25(5):960–971. doi: https://doi.org/10.1093/molbev/msn043.

1743 Shafer, A.B.A., Peart, C.R., Tusso, S., Maayan, I., Brelsford, A., Wheat, C.W., Wolf, J.B.W.,
1744 2017. Bioinformatic processing of RAD-seq data dramatically impacts downstream

1745 population genetic inference. Methods Ecol. Evol. 8:907–917. doi:
1746 https://doi.org.10.1111/2041-210X.12700.

1747 Shi, J.J., Rabosky, D.L., 2015. Speciation dynamics during the global radiation of extant bats.
1748 Evolution, 69(6): 1528-1545. doi: https://doi.org/10.1111/evo.12681.

1749 Simion, P., Delsuc, F., Philippe, H., 2020. To What Extent Current Limits of Phylogenomics
1750 Can Be Overcome? In Scornavacca, C., Delsuc, F., and Galtier, N., editors, Phylogenetics
1751 in the Genomic Era, chapter No. 2.1, pp. 2.1:1–2.1:34. No commercial publisher | Authors
1752 open access book. The book is freely available at https://hal.inria.fr/PGE. HAL Id: hal-
1753 02535366.

1754 Simmons, M.P., 2012. Misleading results of likelihood-based phylogenetic analyses in the
1755 presence of missing data. Cladistics. 28(2): 208-222. doi: https://doi.org/10.1111/j.1096-
1756 0031.2011.00375.x.

1757 Simmons, M.P., Sloan, D.B., Gatesy, J., 2016. The effects of subsampling gene trees on
1758 coalescent methods applied to ancient divergences. Mol. Phylogenet. Evol. 97, 76-89. doi:
1759 https://doi.org/10.1016/j.ympev.2015.12.013.

1760 Smith, B.T., Harvey, M.G., Faircloth, B.C., Glenn, T.C., Brumfield, R.T., 2014. Target capture
1761 and massively parallel sequencing of ultraconserved elements for comparative studies at
1762 shallow evolutionary time scales. Syst. Biol. 63(1)83–95. doi:
1763 https://doi.org/10.1093/sysbio/syt061.

1764 Solís-Lemus, C., Yang, M., Ané, C. 2016. Inconsistency of species tree methods under gene
1765 flow. Syst. Biol. 65(5):843–851. doi: https://doi.org/10.1093/sysbio/syw030.

1766 Song, S., Liu, L., Edwards, S.V., Wu, S. 2012. Resolving conflict in eutherian mammal
1767 phylogeny using phylogenomics and the multispecies coalescent model. P. Natl. Acad. Sci.
1768 USA. 109(37): 14942-14947. doi: https://doi.org/10.1073/pnas.1211733109.

1769 Springer, M.S., Meredith, R.W., Gatesy, J., Emerling, C.A., Park, J., Rabosky, D.L., Stadler,
1770 T., Steiner, C., Ryder, O.A., Janečka, J.E. and Fisher, C.A., 2012. Macroevolutionary
1771 dynamics and historical biogeography of primate diversification inferred from a species
1772 supermatrix. PloS one. 7(11): e49521. doi: https://doi.org/10.1371/journal.pone.0049521.

1773 Springer, M.S., Gatesy, J., 2014. Land plant origins and coalescence confusion. Trends Plant.
1774 Sci. 19(5): 267-269. doi: https://doi.org/10.1016/j.tplants.2014.02.012.

1775 Springer, M.S., Gatesy, J., 2016. The gene tree delusion. Mol. Phylogenet. Evol. 94: 1-33. doi:
1776 https://doi.org/10.1016/j.ympev.2015.07.018.

1777 Springer, M.S., Gatesy,J., 2018. On the importance of homology in the age of phylogenomics.
1778 Syst. Biodivers. 16(3): 210-228. doi: https://doi.org/10.1080/14772000.2017.1401016.

1779 Stamatakis, A., 2014. RAxML version 8: a tool for phylogenetic analysis and post-analysis of
1780 large phylogenies. Bioinformatics. 30(9):1312–1313. doi:
1781 https://doi.org/10.1093/bioinformatics/btu033.

1782 Suchan, T., Pitteloud, C., Gerasimova, N.S., Kostikova, A., Schmid, S., Arrigo, N., Pajkovic,
1783 M., Ronikier, M. and Alvarez, N., 2016. Hybridization capture using RAD probes
1784 (hyRAD), a new tool for performing genomic analyses on collection specimens. PloS one,
1785 11(3). doi: https://doi.org/10.1371/journal.pone.0151651.

1786 Suchan, T., 2018. hyRAD RNA probes preparation and capture. Lab protocol available at:
1787 protocols.io, ID 14096, https://protocols.io/view/hyrad-rna-probes-preparation-and-
1788 capture-rzqd75w.

1789 Suda, J., Kyncl, T., Jarolímová, V., 2005. Genome size variation in Macaronesian angiosperms:
1790 forty percent of the Canarian endemic flora completed. Pl. Syst. Evol. 252(3-4):215–238.
1791 doi: https://doi.org/10.1007/s00606-004-0280-6.

1792 Swofford, D.L., 2003. PAUP*. Phylogenetic analysis using parsimony (*and other methods),
1793 version 4.0a168. Sinauer Associates, Sunderland, Massachusetts, USA

1794 Tan, G., Opitz, L., Schlapbach, R. and Rehrauer, H., 2019. Long fragments achieve lower base
1795 quality in Illumina paired-end sequencing. Sci. Rep. 9(1): pp.1-7. doi:
1796 https://doi.org/10.1038/s41598-019-39076-7.

1797 Uhl, C.H., 1961. The chromosomes of the Sempervivoideae (Crassulaceae). Amer. J. Bot.
1798 48(2):114–123. doi: https://doi.org/10.1002/j.1537-2197.1961.tb11612.x.

1799 Vachaspati, P., Warnow, T., 2015. ASTRID: accurate species trees from internode distances.
1800 BMC genomics, 16(10): 1-13. http://www.biomedcentral.com/1471-2164/16/S10/S3.

1801 Van Der Valk, T., Vezzi, F., Ormestad, M., Dalén, L., Guschanski, K., 2020. Index hopping on
1802 the Illumina HiseqX platform and its consequences for ancient DNA studies. Mol. Ecol.
1803 Resour. 20(5): pp.1171-1181. doi: https://doi.org/10.1111/1755-0998.13009.

1804 van Gurp, T.P., 2017. GBS Barcode Generator. http://www.deenabio.com/services/gbs-adapter
1805 (accessed January 2017).

1806 von Goethe, J.W., 2012. Maximen und reflexionen. Jazzybee Verlag Jürgen Beck. Altenmüster,
1807 Germany. ISBN: 9783849616717.

1808 Wagner, N.D., Gramlich, S., Hörandl, E., 2018. RAD sequencing resolved phylogenetic
1809 relationships in European shrub willows (*Salix* L. subg. *Chamaetia* and subg. *Vetrix*) and
1810 revealed multiple evolution of dwarf shrubs. Ecol Evol. 8(16):8243–8255. doi:
1811 https://doi.org/10.1002/ece3.4360.

1812 Wagner, F., Ott, T., Schall, M., Lautenschlager, U., Vogt, R., Oberprieler, C., 2020. Taming
1813 the Red Bastards: Hybridisation and species delimitation in the Rhodanthemum
1814 arundanum-group (Compositae, Anthemideae). Mol. Phylogenet. Evol. 144, 106702. doi:
1815 https://doi.org/10.1016/j.ympev.2019.106702.

1816 Wang X., Ye X., Zhao L., Li D., Guo Z., Zhuang, H., 2017. Genome-wide RAD sequencing
1817 data provide unprecedented resolution of the phylogeny of temperate bamboos (Poaceae:
1818 Bambusoideae). Sci. Rep. 7:11546. doi: https://doi.org/10.1038/s41598-017-11367-x.

1819 Weitemier, K., Straub, S. C., Cronn, R. C., Fishbein, M., Schmickl, R., McDonnell, A., Liston,
1820 A., 2014. Hyb-Seq: Combining target enrichment and genome skimming for plant
1821 phylogenomics. Appl. Plant Sci. 2(9), 1400042. doi: https://doi.org/10.3732/apps.1400042.

1822 Whitfield, J.B., Lockhart, P.J., 2007. Deciphering ancient rapid radiations. Trends Ecol. Evol.
1823 22(5):258–265. doi: https://doi.org/10.1016/j.tree.2007.01.012.

1824 Wu, S., Song, S., Liu, L., Edwards, S.V., 2013. Reply to Gatesy and Springer: the multispecies
1825 coalescent model can effectively handle recombination and gene tree heterogeneity. P. Natl.
1826 Acad. Sci. USA, 110(13): E1180-E1180. doi: https://doi.org/10.1073/pnas.1300129110.

1827 Xi Z., Liu L., Davis C.C., 2015. Genes with minimal phylogenetic information are problematic
1828 for coalescent analyses when gene tree estimation is biased. Mol. Phylogenet. Evol. 92:63–
1829 71. doi: https://doi.org/10.1016/j.ympev.2015.06.009.

1830 Xi, Z., Liu, L., Davis, C.C., 2016. The impact of missing data on species tree estimation. Molec.
1831 Biol. Evol. 33(3): 838-860. doi: https://doi.org/10.1093/molbev/msv266.

1832 Xu, B., Yang, Z., 2016. Challenges in species tree estimation under the multispecies coalescent
1833 model. Genetics, 204(4), 1353-1368. doi: https://doi.org/10.1534/genetics.116.190173.

1834 Yang, Z., Rannala, B., 2010. Bayesian species delimitation using multilocus sequence data.
1835 Proc. Natl. Acad. Sci. U.S.A. 107(20):9264–9269. doi:
1836 https://doi.org/10.1073/pnas.0913022107.

1837 Yang, Z., 1996. Maximum-likelihood models for combined analyses of multiple sequence data.
1838 J. Mol. Evol. 42(5): 587-596. doi: https://doi.org/10.1007/BF02352289.

1839 Zhang, C., Rabiee, M., Sayyari, E., Mirarab, S., 2018. ASTRAL-III: polynomial time species
1840 tree reconstruction from partially resolved gene trees. BMC Bioinf. 19:153. doi:
1841 https://doi.org/10.1186/s12859-018-2129-y.

1842 Zimmermann, T., Mirarab, S., Warnow, T., 2014. BBCA: Improving the scalability of* BEAST
1843 using random binning. BMC Genomics 15(6):S11. doi: https://doi.org/10.1186/1471-2164-
1844 15-S6-S11.

1845

1846 **Table 1.** The properties of the unfiltered "raw" assembly, the "cleansed" dataset, the datasets
1847 selected by locus filtering and their length truncated variants.

dataset	raw	cleansed	int_251-500	int_301-450	int_251-500_short	int_301-450_short
loci	3,818	3,225	2,788	1,599	2,788	1,599
VAR total	71,691	68,490	56,448	33,480	18,590	10,625
VAR per locus	18.78 (±16.69)	21.24 (±16.82)	20.24 (±15.70)	20.94 (±16.15)	6.67 (±5.65)	6.65 (±5.63)
SNPs total	36,413	33,261	26,533	15,673	8,779	5,040
SNPs per locus	9.54 (±5.25)	10.31 (±9.89)	9.51 (±8.66)	9.80 (±8.86)	3.15 (±3.17)	3.15 (±3.16)
PIS total	35,278	35,229	29,915	17,807	9,811	5,585
PIS per locus	9.24 (±10.73)	10.92 (±10.86)	10.73 (±10.67)	11.14 (±11.05)	3.52 (±3.93)	3.49 (±3.91)
unlinked PICs total	2,723		2,220	1,287		
locus coverage	8.86 (±5.25)	9.37 (±5.45)	9.67 (±5.57)	9.96 (+-5.62)	9.67 (±5.57)	9.96 (+-5.62)
sample coverage	1,166 (±467)		930 (±333)	549 (±204)		
missingness avg. [%]	69.79	67.69	66.66	65.64	66.66	65.64
locus length avg. [nt]	376 (±93)	379 (±93)	360 (±70)	373 (±43)	120 (±23)	123 (±18)

1848

1849 Given are the total number of loci (loci), the total and average values per locus (standard
1850 deviations in parentheses) for the number of variable sites (VAR), single nucleotide
1851 polymorphisms (SNPs), and parsimony informative sites (PIS), the total number of unlinked
1852 PICs as input for SVD inference, and the average locus coverage (samples per locus), sample
1853 coverage (loci per sample), the average proportion of missingness [%] and the average locus
1854 length [nt].

Table 2. Bootstrap support values and concordance factor values and differences of the inferred datasets using CA-ML, CB-SM and SVD.

inference method	CA-ML			CB-SM			SVD		
dataset	raw	int_25 1-500	int_30 1-450	raw	int_25 1-500	int_30 1-450	raw	int_25 1-500	int_30 1-450
BS backbone branches	86.80	99.20	99.20	83.06	90.14	96.70	100	100	100
BS clade branches	94.80	100	99.60	99.92	99.98	99.08	100	100	100
BS within clade branches	93.71	95.29	94.41	80.25	83.92	83.94	100	100	100
BS all branches	92.63	96.89	96.26	84.41	88.05	89.10	100	100	100
CF clade 1	44.4; 69.2; 24.8	44.5; 68.8; 24.4	46.7; 69.4; 22.7	45.4; 69.1; 23.8	45.0; 68.0; 23.0	47.9; 68.7; 20.7	45.6; 70.0; 24.4	44.5; 69.0; 24.6	45.1; 61.3; 16.2
CF clade 2+3	48.1; 62.3; 14.2	48.7; 62.3; 13.6	50.0; 58.5; 8.5	42.6; 72.4; 29.8	43.1; 72.8; 29.7	44.6; 70.0; 25.4	43.2; 72.1; 28.8	41.8; 71.7; 29.9	43.1; 73.7; 30.6
CF clade 4	40.1; 64.1; 24.0	40.5; 64.5; 24.1	42.5; 66.1; 23.6	36.4; 60.1; 23.7	40.9; 65.4; 24.5	42.5; 65.8; 23.3	37.6; 54.4; 16.8	40.9; 63.8; 22.9	36.6; 59.1; 22.6
CF clade 5	17.4; 57.8; 40.5	17.5; 57.8; 40.3	17.4; 58.4; 41.0	16.1; 59.8; 43.7	18.9; 61.0; 42.1	19.9; 61.5; 41.6	18.7; 60.8; 42.1	18.4; 61.7; 43.3	17.3; 60.4; 43.1
CF clade branches	56.2; 83.3; 27.1	55.9; 83.2; 27.3	58.7; 81.7; 22.9	51.5; 80.8; 29.3	55.8; 81.5; 25.7	59.3; 80.2; 20.9	57.6; 83.2; 25.6	54.9; 81.7; 26.8	53.2; 79.2; 26.1
CF backbone branches	58.6; 75.9; 17.3	55.9; 69.5; 13.6	57.9; 71.2; 13.3	55.0; 68.1; 13.1	55.9; 69.6; 13.7	57.9; 71.6; 13.6	49.1; 62.7; 13.6	49.9; 66.7; 16.7	48.9; 64.8; 15.9

Given are the average BS support values (sectional and total) and the average gene (gCF) and site concordance factor (sCF) values (of the within clade branches, the clade branches and backbone branches) of the inferred datasets ("raw", "int_251-500", "int_301-450", "int_251-500_short", "int_301-450_short") using CA-ML, CB-SM and SVD. The average concordance factor (CF) values are shown in this order: gCF; sCF; gCF-sCF-difference.

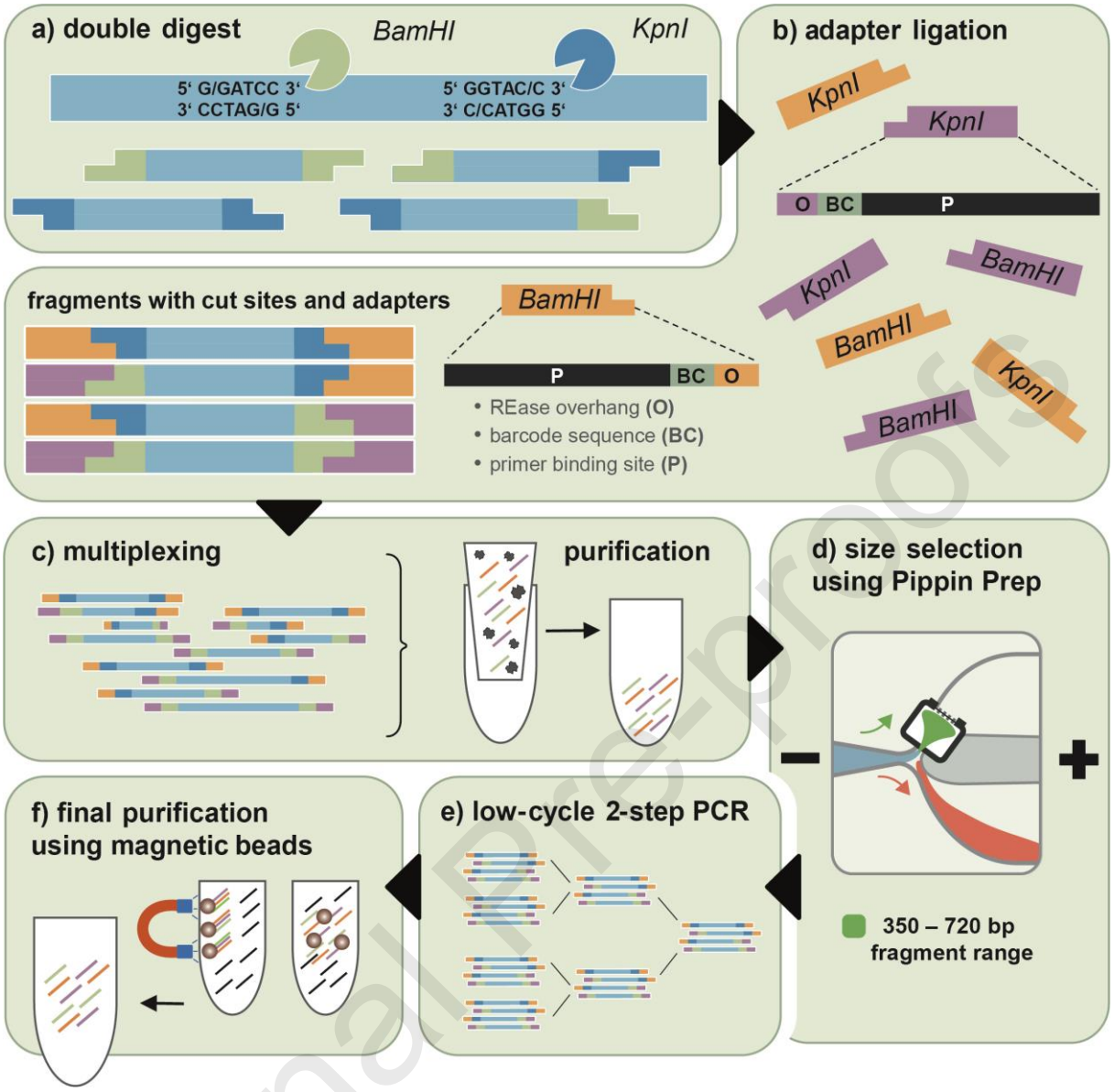

Figure 1. The lab workflow of the modified RADseq protocol consists of six steps (a – f). a) Genomic DNA is digested simultaneously using the REases *BamHI* and *KpnI*. b) Barcode and common adapters are ligated to the fragments. c) The barcoded samples are multiplexed and purified. d) The pool is size selected to a 350 – 720 bp length range using Pippin Prep. e) The size selected pool is amplified using a low-cycle 2-step PCR. f) The final purification using magnetic beads removes PCR and size selection artifacts.

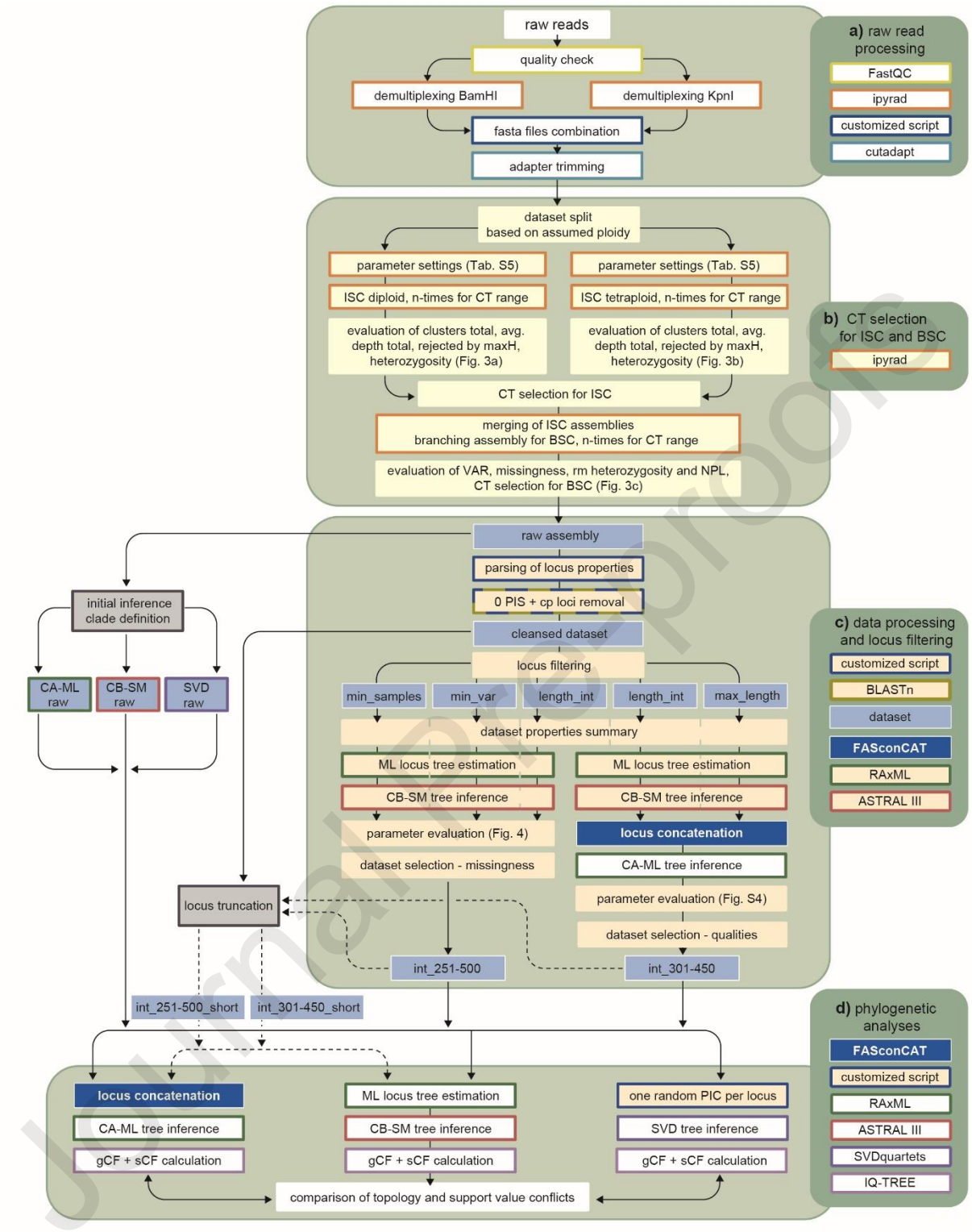

Figure 2. The schematic overview of the data analysis is split into four major parts (a-d, boxes on the right side). The boxes in light blue indicate sub-/datasets. Dashed arrows illustrate parameter applications between datasets. Colored box edges show the software used for the work step. During the raw read processing (a) the quality is assessed using FastQC, the reads are demultiplexed two times with respect to the REase cut sites and the sample specific barcodes, combined into sample fasta files, and adapter and cut sites are removed using cutadapt. For the clustering threshold (CT) selection approach (b), the data set is split based on the assumed ploidy and the *ipyrad* parameters are adjusted as required. For in-sample-clustering (ISC) a CT range of 0.81 – 0.99 is tested for both datasets and *ipyrad* outputs are evaluated with respect to the number of total clusters, total average read depth, clusters rejected by maxH (flagged paralogs) and heterozygosity (Fig. 3a and b). The selected ISC assemblies are merged and branched to test the CT range (see above) for between-sample-clustering (BSC). The resulting assemblies are evaluated with respect to the number of retained loci, the retained sequence variation (VAR), missingness and the number of new polymorphic loci (NPL, Fig. 3c). The selected "raw" assembly is used for initial phylogenetic inference and clade definition (c). The locus properties (locus ID, length, number of samples, number of SNPs, PIS and VAR) are parsed using a customized script. Loci showing no variation and chloroplast loci are removed. The loci of the "cleansed" dataset are filtered into several sub-datasets based on their properties. The first locus filtering approach, using a missingness threshold for dataset selection, resulted in the "int_251-500" dataset. The second filtering approach, using sub-dataset properties and resulting phylogenetic patterns for dataset selection, resulted in the "int_301-450" dataset. The truncated loci of the "raw" assembly were re-arranged based on the selected datasets of the locus filtering (locus truncation, dashed arrows). The datasets ("raw", "int_251-500", "int_301-450" and "short") are used for comparative phylogenetic inference (d). Individual loci are either concatenated using FASconCAT for CA-ML inference or used to calculate ML locus trees as input for CB-SM

inference. The SVD datasets are created by picking a single randomly selected parsimony informative character (PIC) of each locus. To assess the resulting trees of the tested inference methods across datasets, we compared changes in BS support values and gene (gCF) and site concordance factor (sCF) values.

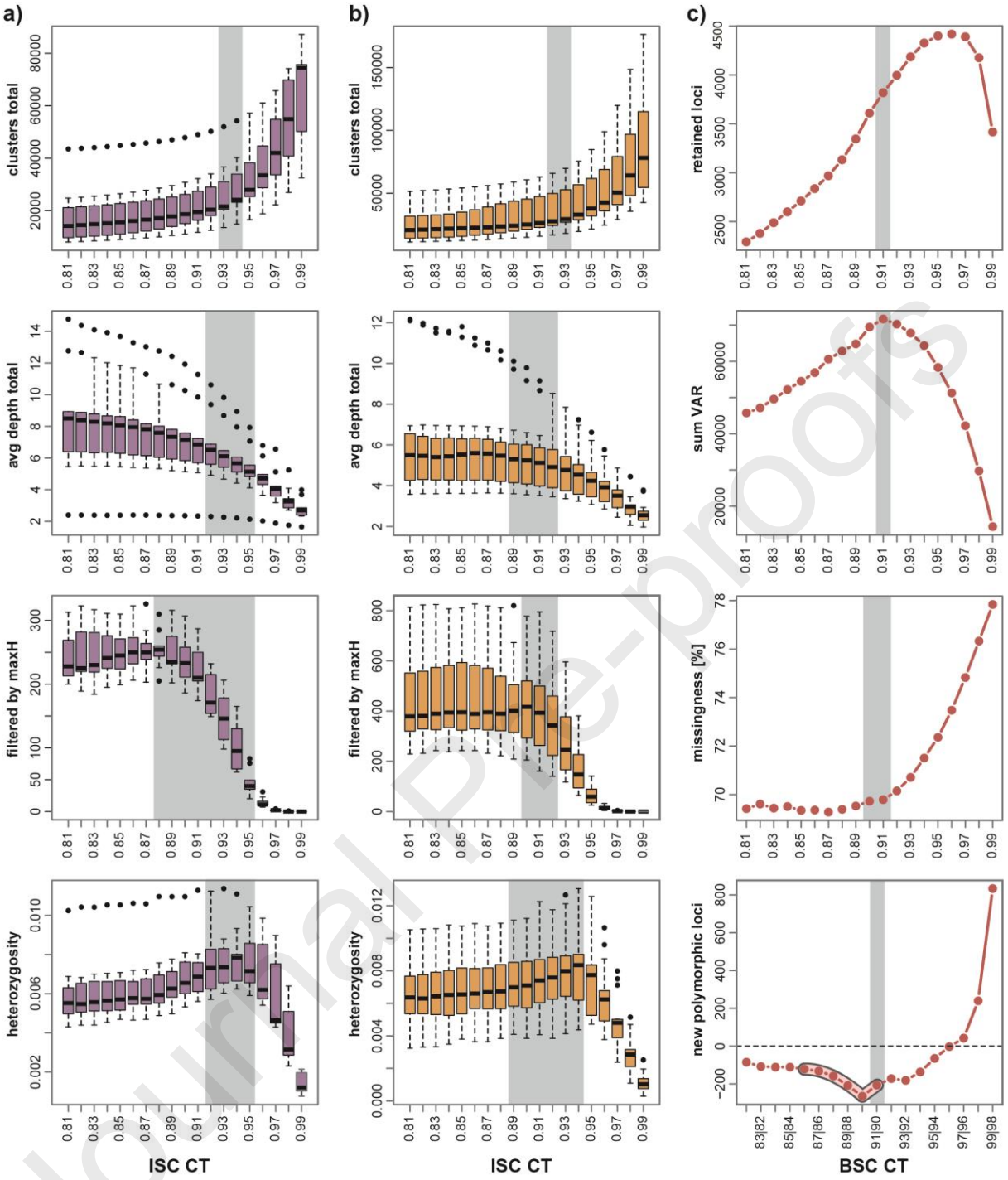

Figure 3. To determine suitable thresholds for in-sample-clustering (ISC) and between-sample-clustering (BSC), trends of several metrics tested across a CT range of 0.81-0.99 were evaluated. For ISC threshold selection of the diploid (a) and tetraploid (b) samples, the number of clusters, the average read depth, flagged paralogs (filtered by maxH) and the allelic variation (heterozygosity) were recorded and plotted. Transition zones from the over- to the undermerging area containing several suitable CTs are shaded in grey. CTs within these zones were averaged to a consensus CT. To select a suitable threshold for clustering between samples of the merged ISC assemblies, the number of retained loci, the retained sequence variation (VAR), the missingness and the number of new polymorphic loci (NPL) were recorded (c). The "hockey stick signal" in the NPL plot, which indicates the assembly containing most accurately clustered sequence variation, is in line with the requirements for the other metrics.

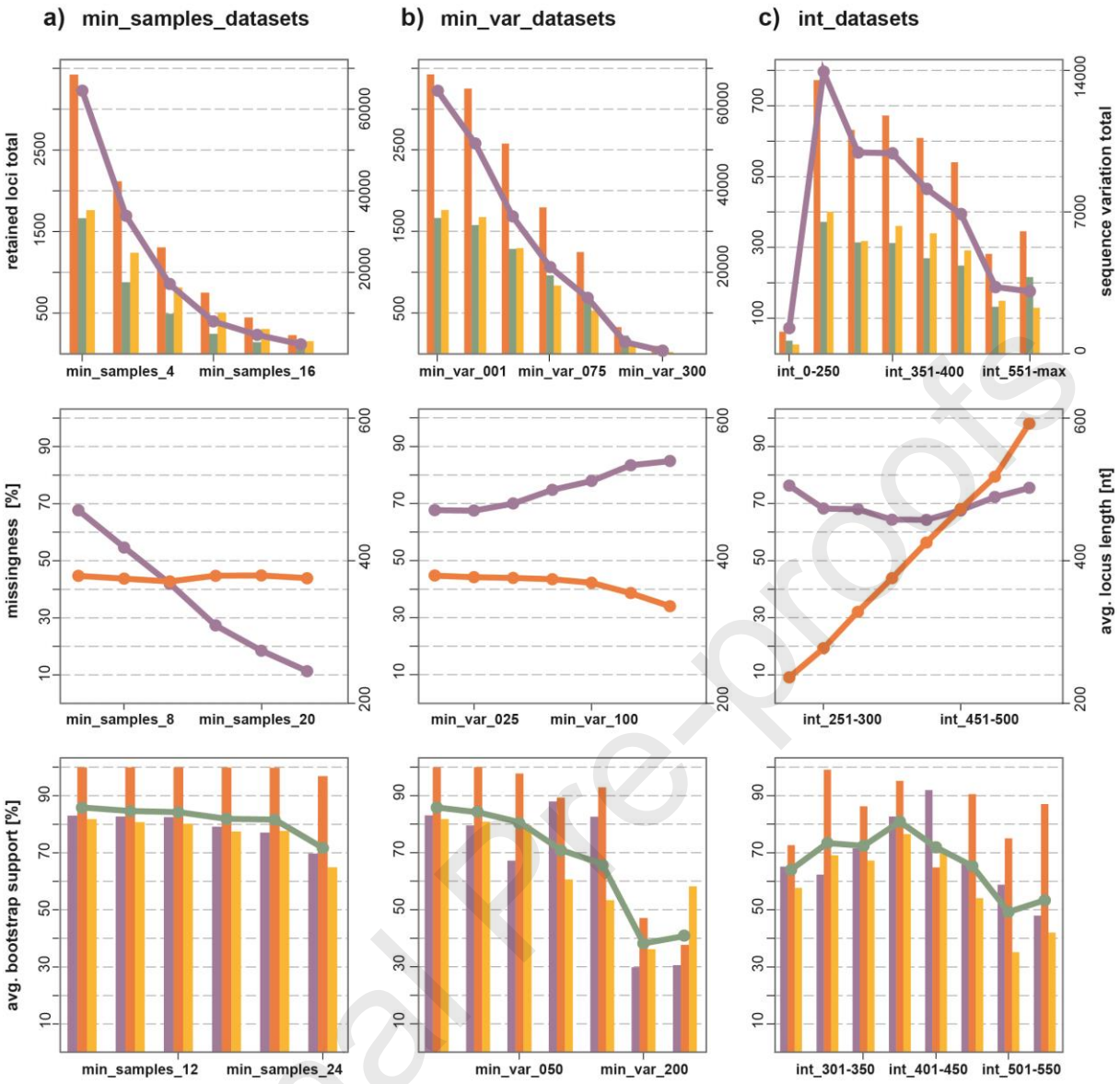

Figure 4. The loci of the „cleansed" assembly were rearranged into sub-datasets based on the minimum number of samples required (a), the minimum variability required (b) and locus length intervals (c). For each sub-dataset, properties such as the number of retained loci (upper plots, purple line with data points), sequence variation (orange=VAR, green=SNPs, yellow=PIS), the average missingness (middle plots, purple line with data points) and average locus length (orange line) were recorded. The average BS support values of the resulting CB-SM trees are given in total (bottom plots, green line with data points) and for the three sections (purple=backbone branches, orange=clade branches, yellow=within clade branches).

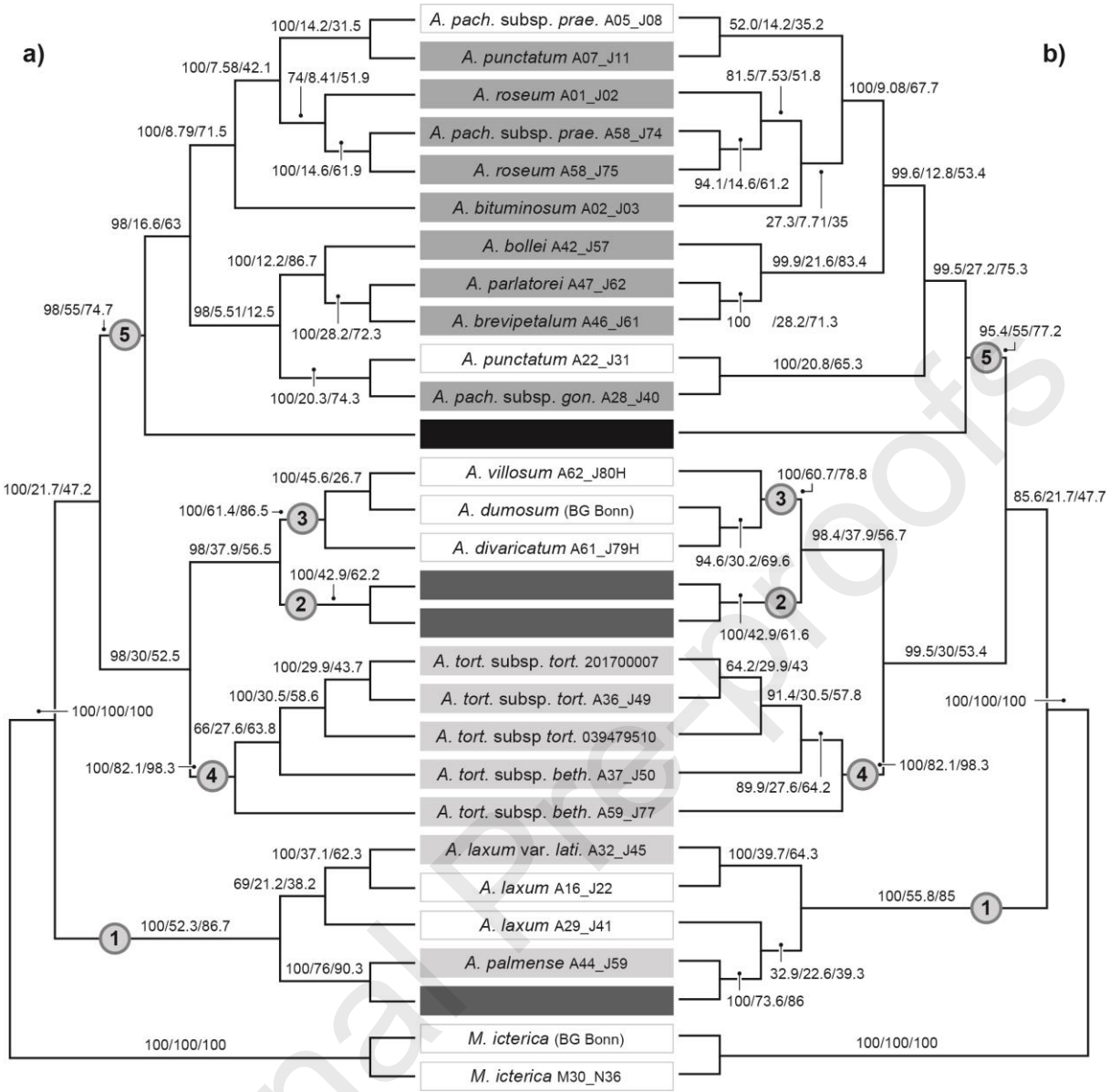

Figure 5. The CA-ML (a) and CB-SM (b) phylogenies of the "int_301-450" dataset. Bootstrap support, gene and site concordance factor values are given above branches. Clades are indicated by the encircled numbers 1-5. Boxes shaded in light and dark gray indicate diploid and tetraploid samples, respectively. The sample *A. porphyrogennetos* A12_J16 showed an intermediate genome size and was treated as tetraploid (black box).

Philipp Hühn: Conceptualization, Methodology, Software, Validation, Formal analysis, Investigation, Data Curation, Writing - Original Draft, Visualization, Project administration, Supervision

Markus S. Dillenberger: Methodology, Software, Formal analysis, Writing - Review & Editing

Michael Gerschwitz-Eidt: Methodology, Software, Formal analysis, Writing - Review & Editing

Elvira Hörandl: Resources, Writing - Review & Editing

Jessica A. Los: Investigation, Resources

Thibaud F.E. Messcherschmid: Investigation, Resources

Claudia Paetzold: Methodology, Writing - Review & Editing

Benjamin Rieger: Methodology, Software

Gudrun Kadereit: Conceptualization, Resources, Writing - Review & Editing, Supervision, Funding acquisition

- Modified RADseq protocol yields strongly reduced number of length extended loci
- Evaluation of assembly metrics eases clustering threshold selection using ipyrad
- Locus filtering by length facilitates detection of biased data
- Dataset reduction improves overall data quality
- Informative RADseq loci support coalescent-based phylogenetic inference with ASTRAL

Graphical Abstract